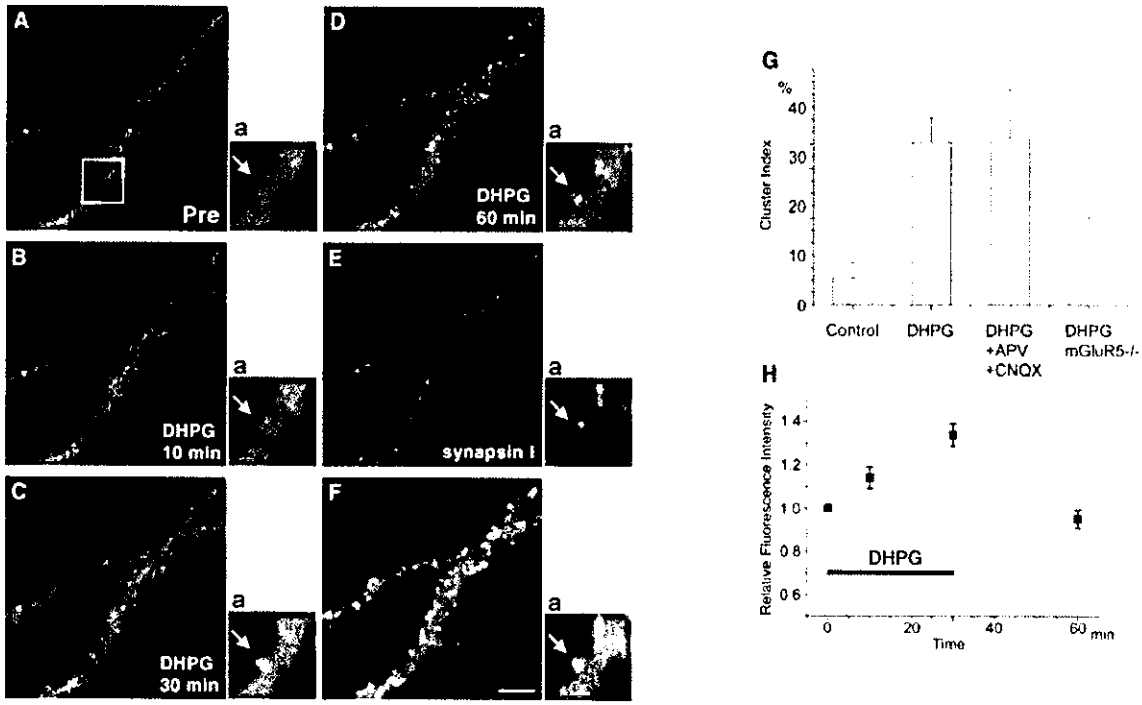

Figure 3. TLS Localization to the Postsynaptic Spines Is Dependent on mGluR Signals

(A–F) Time-lapse recording of TLS-GFP clusters after DHPG treatment (100 μM, 60 min) reveals that TLS-GFP accumulates within spines. (Aa–Fa) High-magnification view of the same area shown as a white rectangle in (A). Accumulation of TLS-GFP clusters takes place at the sites where retrospective immunocytochemistry by anti-synapsin I reveals the presence of presynaptic structures (E and F). Photos (F) and (Fa) are merged images of (D)–(E) and (Da)–(Ea), respectively.

(G and H) The average cluster index (the increase % of relative fluorescence intensity after the stimulation divided by the relative fluorescence intensity before the stimulation) is increased in cells treated with DHPG (n = 26). This DHPG-dependent effect does not change even in the combined presence of APV and CNQX (n = 7). The DHPG-dependent spine accumulation is abolished in hippocampal neurons from mGluR5$^{-/-}$ (n = 10). Control, n = 17 (H) DHPG (100 μM) induces accumulation of TLS-GFP in spines. However, upon the removal of DHPG 30 min after the start of treatment, the amount of TLS-GFP in spines returns to the control level. Error bars in (G) and (H) indicate SEM (n = 20).

3G). DHPG treatment did not change the number of the spines protruding from the shaft under the experimental conditions used nor caused significant elongation of the spines. Moreover, upon the removal of DHPG 30 min after the treatment, the number of spines containing TLS-GFP clusters moved back to the control level after another 30-min period of incubation (Figure 3H). This result clearly indicates that the spine localization induced by DHPG is a reversible event and that the spine localization was dependent on the state of mGluR activation. Hippocampal neurons expressing TLS-GFP were exposed to DHPG in the presence of both CNQX and APV, which are antagonists for the AMPA/kainate-type glutamate receptor (GluR) and NMDA receptor (NMDAR), respectively, to identify the signals responsible for the spine localization. The combination of CNQX and APV did not affect the DHPG-induced spine localization of TLS (Figure 3G), indicating that the spine localization was solely mediated by the mGluR activation and was independent of GluR or NMDAR activation. Because we demonstrated that TLS accumulated exclusively in the spines of postsynaptic neurons (Figure S1D–S1F), mGluR5, the major group 1 mGluR, was suspected to be the most plausible receptor candidate involved in TLS localization to the spines of pyramidal neurons in the CA1 area. To test this possibility, we examined the DHPG-induced TLS redistribution in hippocampal neurons derived from mGluR5 knockout mice [16]. In neurons of the mGluR5 homozygous mutants in which basal TLS distribution was not changed compared with wild-type (Figure S4), DHPG could not induce spine localization of TLS (Figure 3G). These results confirm that TLS accumulation in spines is induced upon postsynaptic activation of signaling cascades initiated by mGluR5.

Abnormal Spine Morphology in TLS-Deficient Mice

To investigate the context of TLS localization and its role in neuronal development, we prepared primary hippocampal neurons from embryos of TLS mutant mice (TLS$^{-/-}$) [17] and stained them with the lipophilic dye DiI (Figure 4). In the hippocampal neurons from the TLS-deficient mice, the dendrites were irregularly branched, and numerous long and thin processes like immature axons extended from the cell body (Figure 4A, arrows in upper panel of −/−), which is not observed in wild-type neurons extended with a single axon from the cell body (Figure 4A, arrows in upper panel of +/+). How-

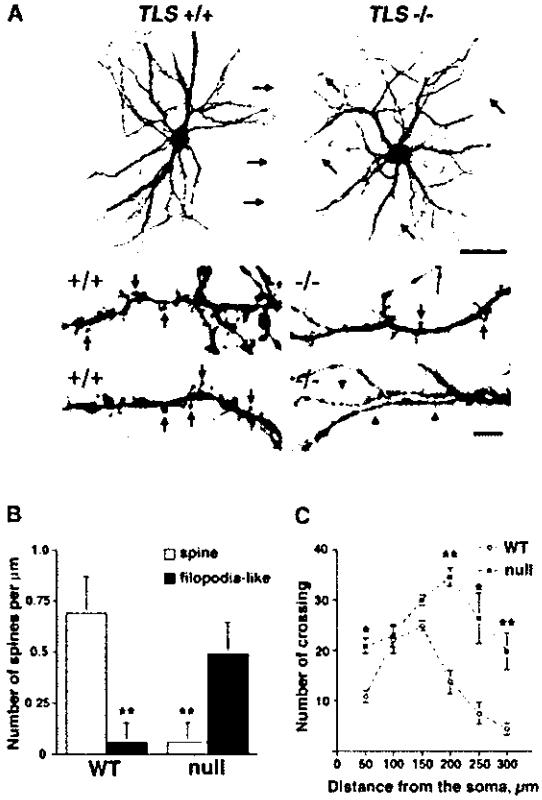

Figure 4. TLS-Deficient Mice Show Reduced Spine Number and Abnormal Spine Morphology

(A) Morphology of hippocampal neurons from TLS wild-type (*TLS*$^{+/+}$) and TLS null mutant (*TLS*$^{-/-}$) mice visualized by application of lipophilic dye DiI at 21 days in vitro. In neurons obtained from TLS$^{-/-}$ mice, there were multiple axon-like processes that have elongated from the soma (arrows in −/− of the upper panel). With higher magnification, the spines were reduced in their number (arrows in −/− of the middle panel) or transformed into thin cytoplasmic protrusion similar to filopodia (arrowheads in −/− of the lower panel). In contrast, majority of dendritic protrusions in wild-type neurons showed the morphology of mushroom-shaped spines, containing large heads connected to the shaft via thin neck (arrows in +/+ of the lower panels). Scale bars, 50 μm in upper panels and 5 μm in lower panels.

(B) Quantitative analysis of spine density in hippocampal neurons taken from wild-type (+/+) and TLS null mutant (−/−) mice. There was a significant decrease of spine density in the TLS null mice. On the other hand, the number of filopodia-like protrusions was significantly increased in TLS null neurons (50 representative dendrites from 10 neurons with each genotype were measured; double asterisk, $p < 0.01$). Error bars, SEM.

(C) Sholl profiles revealed a slight change in branching pattern of TLS null cultured pyramidal neurons. Number of dendritic crossings within 50 μm and over 200 μm from the soma significantly increased in TLS null neurons (n = 30 independent neurons). Asterisk, $p < 0.05$; double asterisk, $p < 0.01$.

ever, immunostaining for MAP2 or SMI31 revealed that TLS-null neurons possessed multiple dendrites and a single axon, indicating that the neuronal polarity was not affected by the TLS deficiency (data not shown). The spines in TLS-deficient neurons were reduced in number (Figure 4A, arrows in lower panel of −/−) or transformed into thin and long cytoplasmic protrusions similar to filopodia (Figure 4A, arrowheads in lower panel of −/−). Their structure was distinct from that of the wild-type hippocampal neuron spines, which displayed thin necks and relatively large heads and, thus, had a mushroom-like shape (Figure 4A, arrows in lower panel of +/+) [1]. Quantitative analysis revealed that the density of spines in TLS-deficient neurons was significantly reduced compared with that in the wild-type ones (Figure 4B). On one hand, the number of filopodia-like spines was increased in TLS-deficient neurons. To clarify further the difference in spine morphology between the TLS-deficient and wild-type neurons, we measured dendritic complexity by a standard Sholl analysis [18], which counts the number of dendritic crossings at 50 μm concentric circles. There were more branches in the proximal and distal region in TLS-deficient neurons compared with those in wild-type (Figure 4C). In the proximal region, more dendrites were elongated directly from the soma in the TLS null neurons. It appeared that there were more tertiary dendritic branches in the distal region of the TLS null neurons. These data imply a key role for TLS in neuronal maturation including dendritic branching and also maintenance of spine stability.

Discussion

Metabotropic glutamate receptors have diverse functions in signal transduction of neurons. Group 1 mGluRs, including mGluR1 and mGluR5, are localized at the periphery of the postsynaptic junctional membrane of principal neurons in the hippocampus and the cerebellum [19, 20]. Our time-lapse recording of TLS-GFP revealed that treatment with DHPG, a selective group 1 mGluR agonist, increased the amount of TLS-GFP clusters in the spines of mature dendrites within 30 min of stimulation (Figure 3). By using hippocampal neurons from mGluR5 knockout mice, we showed that postsynaptic mGluR5-mediated signaling system was responsible for the translocation of TLS. The reversal of TLS translocation after DHPG washout, shown in Figure 3H, clearly indicates that accumulation of TLS in spines was maintained by mGluR activity and not stabilized by other molecular interactions. Activated postsynaptic mGluR5 can induce increases in both intracellular calcium concentration $[Ca^{2+}]i$ and PKC activation through the G protein-linked inositol phospholipids pathway [21]. On the other hand, PKC activation has been shown to control the redistribution of a wide variety of proteins localized in the postsynaptic density (PSD) [22, 23]. Because PKC is responsible for the reorganization of the actin cytoskeleton in a variety of cell types [24], activation of PKC by mGluR5 may subsequently release TLS-containing RNA granules from their actin bound state and initiate their translocation into spines. This hypothesis can be tested by experiments with multiple fluorescent reporters to simultaneously monitor translocation of TLS and reorganization of the actin cytoskeleton.

Although DHPG treatment induces accumulation of TLS, signaling via mGluR5 cannot be the sole mechanism of TLS accumulation in spines. The presence of

another signaling system is evident from phenotypic examination of cultured neurons from mGluR5 null mice, where transition of TLS from dendritic shafts to spines took place with a time course similar to that for wild-type mice (unpublished data). On the other hand, absence of TLS in hippocampal neurons affected the morphology of the dendrites and reduced the number of the spines (Figure 4). It is likely that accumulation of TLS into spines is essential for their structural maturation but is dependent on multiple signaling systems including mGluR5 activation. Abnormal spine morphology has also been reported in FMRP null mice [25, 26]. In the FMRP knockout mice, neuronal dendrites exhibited long and thin dendritic spines with increased density. This increased spine density may be attributed to the absence of an activity-dependent translational suppression by FMRP [27]. The contrasting phenotypes of these null mutants illustrate the functional diversity of RNA binding proteins in dendrites.

Considering the dual functions of TLS as the RNA-splicing factor and an RNA transporter, we may speculate that TLS may coordinately regulate the rate of RNA splicing in the nucleus and the amount of mRNA transported to local translational machinery in spines in response to synaptic activation. Understanding how postsynaptic metabotropic signals regulate TLS dynamics will be essential in order to decipher the complex cellular system that integrates synaptic activity, RNA splicing and transport, and local dendritic translation. Our present and future findings on the neuronal functions of TLS do and will provide important keys for further understanding the molecular basis of synaptic plasticity and a general insight into local translation in polarized cells.

Supplemental Data

Supplemental Data include four figures, two movies, and Supplemental Experimental Procedures and are available with this article online at http://www.current-biology.com/cgi/content/full/15/6/587/DC1/.

Acknowledgments

We thank M. Kuno, T. Manabe, and H. Sabe for their helpful discussions. We greatly thank D. Ron and E. Schuman for the human TLS and the rat Staufen cDNA clones, respectively. We appreciate T. Ebihara and K. Sobue for kindly providing us CortBP antibody and J. Roder for the generous contribution of mGluR5-null mice. Finally, we thank Y. Sakakida and Y. Watanabe for mouse maintenance as well as K. Hamajima, I. Kawabata, and N. Takashima for their help with preparing the primary cultures of neurons. This work was supported in part by grants from the Ministry of Education, Culture, Sports, Science and Technology, Mitsubishi Pharma Research Foundation, Senri Life Science Foundation, and Sony Corporation. G.G.H. was supported by grants from the National Cancer Institute of Canada.

Received: September 1, 2004
Revised: January 5, 2005
Accepted: January 5, 2005
Published: March 29, 2005

References

1. Hering, H., and Sheng, M. (2001). Dendritic spines: structure, dynamics and regulation. Nat. Rev. Neurosci. *2*, 880–888.
2. Kiebler, M.A., and DesGroseillers, L. (2000). Molecular insights into mRNA transport and local translation in the mammalian nervous system. Neuron *25*, 19–28.
3. Job, C., and Eberwine, J. (2001). Localization and translation of mRNA in dendrites and axons. Nat. Rev. Neurosci. *2*, 889–898.
4. Steward, O., and Schuman, E.M. (2001). Protein synthesis at synaptic sites on dendrites. Annu. Rev. Neurosci. *24*, 299–325.
5. Steward, O., and Schuman, E.M. (2003). Compartmentalized synthesis and degradation of proteins in neurons. Neuron *40*, 347–359.
6. Crozat, A., Aman, P., Mandahl, N., and Ron, D. (1993). Fusion of CHOP to a novel RNA-binding protein in human myxoid liposarcoma. Nature *363*, 640–644.
7. Iko, Y., Kodama, T.S., Kasai, N., Oyama, T., Morita, E.H., Muto, T., Okumura, M., Fujii, R., Takumi, T., Tate, S., et al. (2004). Domain architectures and characterization of an RNA-binding protein, TLS. J. Biol. Chem. *279*, 44834–44840.
8. Zinszner, H., Sok, J., Immanuel, D., Yin, Y., and Ron, D. (1997). TLS (FUS) binds RNA in vivo and engages in nucleo-cytoplasmic shuttling. J. Cell Sci. *110*, 1741–1750.
9. de Hoog, C.L., Foster, L.J., and Mann, M. (2004). RNA and RNA binding proteins participate in early stages of cell spreading through spreading initiation centers. Cell *117*, 649–662.
10. Husi, H., Ward, M.A., Choudhary, J.S., Blackstock, W.P., and Grant, S.G. (2000). Proteomic analysis of NMDA receptor-adhesion protein signaling complexes. Nat. Neurosci. *3*, 661–669.
11. Kanai, Y., Dohmae, N., and Hirokawa, N. (2004). Kinesin transports RNA; isolation and characterization of an RNA-transporting granule. Neuron *43*, 513–525.
12. Kohrmann, M., Luo, M., Kaether, C., DesGroseillers, L., Dotti, C.G., and Kiebler, M.A. (1999). Microtubule-dependent recruitment of Staufen-green fluorescent protein into large RNA-containing granules and subsequent dendritic transport in living hippocampal neurons. Mol. Biol. Cell *10*, 2945–2953.
13. Tang, S.J., Meulemans, D., Vazquez, L., Colaco, N., and Schuman, E. (2001). A role for a rat homolog of staufen in the transport of RNA to neuronal dendrites. Neuron *32*, 463–475.
14. Kang, H., and Schuman, E.M. (1996). A requirement for local protein synthesis in neurotrophin-induced hippocampal synaptic plasticity. Science *273*, 1402–1406.
15. Schratt, G.M., Nigh, E.A., Chen, W.G., Hu, L., and Greenberg, M.E. (2004). BDNF regulates the translation of a select group of mRNAs by a mammalian target of rapamycin-phosphatidylinositol 3-kinase-dependent pathway during neuronal development. J. Neurosci. *24*, 7366–7377.
16. Lu, Y.M., Jia, Z., Janus, C., Henderson, J.T., Gerlai, R., Wojtowicz, J.M., and Roder, J.C. (1997). Mice lacking metabotropic glutamate receptor 5 show impaired learning and reduced CA1 long-term potentiation (LTP) but normal CA3 LTP. J. Neurosci. *17*, 5196–5205.
17. Hicks, G.G., Singh, N., Nashabi, A., Mai, S., Bozek, G., Klewes, L., Arapovic, D., White, E.K., Koury, M.J., Oltz, E.M., et al. (2000). Fus deficiency in mice results in defective B-lymphocyte development and activation, high levels of chromosomal instability and perinatal death. Nat. Genet. *24*, 175–179.
18. Sholl, D.A. (1953). Dendritic organization in the neurons of the visual and motor cortices of the cat. J. Anat. *87*, 387–406.
19. Baude, A., Nusser, Z., Roberts, J.D., Mulvihill, E., McIlhinney, R.A., and Somogyi, P. (1993). The metabotropic glutamate receptor (mGluR1 alpha) is concentrated at perisynaptic membrane of neuronal subpopulations as detected by immunogold reaction. Neuron *11*, 771–787.
20. Shigemoto, R., Nomura, S., Ohishi, H., Sugihara, H., Nakanishi, S., and Mizuno, N. (1993). Immunohistochemical localization of a metabotropic glutamate receptor, mGluR5, in the rat brain. Neurosci. Lett. *163*, 53–57.
21. Nakanishi, S. (1994). Metabotropic glutamate receptors: synaptic transmission, modulation, and plasticity. Neuron *13*, 1031–1037.
22. Fong, D.K., Rao, A., Crump, F.T., and Craig, A.M. (2002). Rapid synaptic remodeling by protein kinase C: reciprocal translocation of NMDA receptors and calcium/calmodulin-dependent kinase II. J. Neurosci. *22*, 2153–2164.
23. Lan, J.Y., Skeberdis, V.A., Jover, T., Grooms, S.Y., Lin, Y., Ar-

aneda, R.C., Zheng, X., Bennett, M.V., and Zukin, R.S. (2001). Protein kinase C modulates NMDA receptor trafficking and gating. Nat. Neurosci. *4*, 382–390.

24. Keenan, C., and Kelleher, D. (1998). Protein kinase C and the cytoskeleton. Cell. Signal. *10*, 225–232.
25. Comery, T.A., Harris, J.B., Willems, P.J., Oostra, B.A., Irwin, S.A., Weiler, I.J., and Greenough, W.T. (1997). Abnormal dendritic spines in fragile X knockout mice: maturation and pruning deficits. Proc. Natl. Acad. Sci. USA *94*, 5401–5404.
26. Nimchinsky, E.A., Oberlander, A.M., and Svoboda, K. (2001). Abnormal development of dendritic spines in FMR1 knock-out mice. J. Neurosci. *21*, 5139–5146.
27. Antar, L.N., and Bassell, G.J. (2003). Sunrise at the synapse: the FMRP mRNP shaping the synaptic interface. Neuron *37*, 555–558.

European Journal of Neuroscience, Vol. 20, pp. 2909–2916, 2004

Fez1 is layer-specifically expressed in the adult mouse neocortex

Kiyoshi Inoue,[1] Toshio Terashima,[2] Toru Nishikawa[3] and Toru Takumi[1]
[1]Osaka Bioscience Institute, Suita, Osaka 565-0874, Japan
[2]Department of Anatomy and Neurobiology, Kobe University Graduate School of Medicine, Kobe 650-0017, Japan
[3]Division of Psychiatry and Behavioural Sciences, Tokyo Medical and Dental University Graduate School, Tokyo 113-8519, Japan

Keywords: cerebral patterning, *in situ* hybridization, microarray, pyramidal neuron, zinc-finger

Abstract

The mammalian cerebral neocortex occupies the largest area of the cerebral cortex and is cytoarchitectually composed of six layers (I–VI). Recent molecular analysis has begun to reveal the existence of various developmental programs, including the genetic regulation of arealization of the neocortex. Although an increasing number of molecular determinants of the developmental stages of the neocortex have been identified, no genes specifically expressed in the adult neocortex have been identified to date. By global screening using microarrays, combined with systematic *in situ* hybridization, we identified a zinc-finger type transcription factor, Fez1, which is expressed predominantly in the mouse adult neocortex. No other genes in the neocortex have been shown to date to have their expression with such high specificity. Using two-color *in situ* hybridization, we show that Fez1 is mainly expressed in cortical layers V and VI, not in γ-aminobutyric acid neurons but in pyramidal neurons, the projection neurons of the cerebral cortex. Immunohistochemistry also shows that Fez1 is expressed in deep layers of the neocortex. Fez1 will be invaluable not only for the molecular understanding of corticogenesis but also for understanding the physiological functions of the adult neocortex, as well as for the use of its promoter in gene-manipulated animals and in conditional expression systems.

Introduction

The cerebral neocortex occupies the largest region of the mammalian telencephalon. Its volume evolutionally increases in relation to complexity of cognitive behavior and, thus, the proportion of the neocortex to the brain is the highest in humans among all organisms. Much of modern neuroscience has been directed towards understanding the functions and disorders of the human cortex (Kandel *et al.*, 2000). The neocortex, concerned with cognitive functioning, is composed of an enormous number of neurons and has six layers (I–VI). The majority of cortical neurons are pyramidal cells found in all layers except layer I. These pyramidal cells are the projection neurons that utilize the excitatory neurotransmitters glutamate and aspartate (Chan *et al.*, 2001). The remaining neurons that are scattered in all layers are interneurons which utilize the inhibitory γ-aminobutyric acid (GABA) and neuropeptides. Information in the neocortex is processed across the layers via an interconnected set of neurons called columns. Many neurological diseases including mental illnesses are due to the dysfunction of the neocortex.

Brain regionalization and cerebral patterning are intriguing issues, and two classical models, the protomap model (Rakic, 1988) and the protocortex model (O'Leary, 1989), have dominated research into the development of the cortical area map. The former theory is based on the idea that intrinsic regional differences are established within the neuroepithelium by molecular determinants that regulate neocortical areal specification, including the targeting of thalamic axons. The latter one is based on the idea that regionalization is induced by extrinsic cues, in particular by incoming thalamic axons, which convey positional and functional specification. Recent molecular biological techniques have begun to unveil the complex development of the cerebral cortex and its mechanism (O'Leary & Nakagawa, 2002; Garel *et al.*, 2003; Grove & Fukuchi-Shimogori, 2003). For example, the graded expression of the transcription factors, Emx2 and Pax6, in the neuroepithelium was found to be responsible for the formation of neocortical areas with the correct size proportion. Furthermore, the graded expression of these transcription factors was found to be sufficient to stably activate morphogenesis of the cerebral cortex and to repress that of adjacent structures, such as the striatum (Muzio *et al.*, 2002). The isolation and characterization of regionally expressed genes have provided useful markers and candidates for genes that may control tissue- or region-specific identity (Chenn *et al.*, 1997). Many molecular determinants including the above required for the development of the neocortex have been reported; however, no genes expressed specifically in the adult neocortex have been reported so far.

Identification of a neocortex-specific gene is important not only because it may play a key role in the development or physiological functioning of the cerebral neocortex, but also because its promoter region can be used to control neocortex-specific expression of any kind of genes of interest. Two kinds of promoters, CaMKIIα and Emx1, have been used to date for the creation of transgenic mice which express the transgene predominantly in the neocortex. However, the expression of both of these promoters is not strictly confined to the neocortex. Besides the neocortex, CaMKIIα is widely expressed in the forebrain, and strongly in the hippocampus and striatum (Erondu & Kennedy, 1985; Burgin *et al.*, 1990). Although Emx1 is expressed more specifically in the cerebral cortex than CaMKIIα, strong expression is observed in the hippocampus and the olfactory bulb as well as in peripheral tissues such as the kidney (Briata *et al.*,

Correspondence: Dr T. Takumi, as above.
E-mail: takumi@obi.or.jp

Received 24 April 2004, revised 18 August 2004, accepted 22 September 2004

doi:10.1111/j.1460-9568.2004.03763.x

1996). As described above, no genes have previously been identified that are specifically expressed in the neocortex.

Here we describe Fez1, a putative transcription factor containing zinc-finger motifs, which we identified through a microarray analysis of genes that are primarily expressed in the adult neocortex, combined with systematic *in situ* hybridization. Although slight mRNA expression was seen in the hypothalamus, the expression of Fez1 is highly enriched in the cerebral neocortex. Using two-color double-labeling *in situ* hybridization, we show that Fez1 is exclusively expressed in cortical layers V and VI, and its expression is not restricted to GABA neurons, but pyramidal neurons, the projection neurons of the cerebral cortex.

Materials and methods

Identification of Fez1

Young adult mice (C57BL/6N) were killed humanely by cervical dislocation, and their brains were removed and separated into the neocortex and the rest of the brain regions, immediately frozen in liquid nitrogen, and stored at −70 °C. Total RNA was extracted from individual tissues using Trizol (GibcoBRL) and poly $(A)^+$ RNA was isolated using the μMACS mRNA Isolation Kit (Miltenyi Biotec GmbH). Five micrograms of poly $(A)^+$ RNA was used for analysis with the Affymetrix Murine 6500 array and Mu 19K (subsets A, B and C) oligonucleotide arrays (Takumi *et al.*, in preparation). Twenty-nine (0.15%) mouse ESTs and 22 (0.34%) known genes, which were expressed at least fivefold (in the case of Mu 19K) and 2.5-fold (in the case of Murine 6500) higher in the neocortex than in the rest of the brain regions, were chosen for second screening using systematic *in situ* hybridization. Of the 39 candidate genes, Fez1 was found to be expressed exclusively in the cortex. All protocols of experiments using animals in this study were approved by the OBI (Osaka Bioscience Institute) Animal Research Committee.

In situ *hybridization*

Adult and postnatal day 0 and 7 male mice and embryonic ICR mice purchased from Japan SLC (Hamamatsu, Japan) were used after being anesthetized with 0.1 mg/g pentobarbital sodium. Template DNAs for probes were synthesized by polymerase chain reaction (PCR) using specific primers and mouse brain cDNA or plasmids provided by RIKEN (The RIKEN Genome Exploration Research Group Phase II Team and the FANTOM Consortium, 2001). For Fez1, ^{35}S-labeled, digoxigenin (DIG)-labeled RNA probes were synthesized by *in vitro* transcription using two independent sequences (the sequence corresponding to the nucleotides 357–914 and 1449–1805) as templates. In addition, sense probes for each of the templates were synthesized as negative controls.

For the ^{35}S-labeled probes, brains were freshly frozen and 16-μm cryosections were fixed in 4% paraformaldehyde in 0.1 M phosphate buffer (PB) pH 7.4, treated with proteinase K (10 μg/mL) for 2 min and postfixed in the same fixative, acetylated with acetic anhydride, dehydrated in ascending alcohol series and air-dried. The sections were incubated for 12 h at 55 °C in hybridization buffer (50% formamide, 0.3 M NaCl, 20 mM Tris–HCl, 10% dextran sulfate, 1 × Denhardt's solution, 500 μg/mL yeast tRNA, 20 mM dithiothreitol and 200 μg/mL herring sperm DNA) containing one of the ^{35}S-labeled cRNA probes. After hybridization, sections were washed with 50% formamide/2 × standard sodium citrate (SSC) at 65 °C and incubated with 1 μg/mL RNase A in RNase buffer (0.5 M NaCl, 10 mM Tris–HCl, 1 mM EDTA pH 8.0) for 30 min at 37 °C. After rinsing with RNase buffer, sections were washed in 50% formamide/2 × SSC at 65 °C, rinsed with 2 × SSC and 0.1 × SSC, dehydrated in alcohol and air-dried. The slides were exposed to Kodak BioMax MR film for 1 week. Films were developed, and black and white images of mRNA expression were obtained. The slides were then coated with Kodak NTB-2 emulsion diluted 1 : 1 with water. Sections were exposed at 4 °C for 4 weeks, developed in Kodak D-19 and counterstained with hematoxylin.

Immunohistochemistry

Male adult ICR mice weighing 25–35 g were deeply anesthetized with 0.1 mg/g sodium pentobarbital and were perfused transcardially with PBS, followed by 4% paraformaldehyde and 0.2% picric acid in 0.1 M PB. After perfusion, the brains were postfixed for 6 h at 4 °C in the same fixative and were transferred to 20% sucrose in 0.1 M PB for 48 h at 4 °C, then were sectioned on a freezing microtome at 50 μm. The slices were stored in PBS containing 0.02% sodium azide at 4 °C until used. Free-floating sections were washed with PBS to remove any sodium azide and were incubated with Fez1 antibody raised against the peptide CTATPSAKDLARTVQS (Immuno-Biological Laboratories, Fujioka, Japan), which is diluted at a ratio of 1 : 300 in 0.1 M PBS containing 0.2% Triton-X100, 5% normal goat serum for 24 h at 4 °C. The sections were then washed three times in PBS, followed by 4 h incubation with fluorescent-conjugated secondary antibody (Alexa 568 goat anti-rabbit, Molecular Probe, 1 : 1000 in 0.1 M PBS containing 0.2% Triton-X100, 5% normal goat serum) at room temperature and were rinsed with PBS and mounted onto slides using an anti-fade mounting medium (Vectashield, VECTOR).

Two-color double-labeling in situ *hybridization*

For two-color double-labeling *in situ* hybridization, a DIG-labeled Fez1 probe and biotin-labeled GAD67 or CaMKIIα probes were used. Mice were perfused with 4% paraformaldehyde/PB and their brains were immersed in fixative for 8 h and in 30% sucrose/PB for 2 days. Ten-micrometre cryosections were fixed in 4% paraformaldehyde/PB, treated with proteinase K (5 μg/mL) for 2 min and washed with 2 mg/mL glycine/PBST (phosphate-buffered saline, 0.1% Tween-20). The sections were then postfixed in 4% paraformaldehyde/0.2% glutaraldehyde/PBST. The sections were incubated with prehybridization buffer (50% formamide, 5 × SSC pH 4.5, 50 μg/mL yeast tRNA, 1% SDS and 50 μg/mL heparin) at 70 °C for 1 h and with prehybridization buffer containing 500 ng/mL DIG-labeled and biotin-labeled probes at 70 °C overnight. The sections were then washed with Solution I (50% formamide, 5 × SSC pH 4.5, 1% SDS) at 70 °C, and Solution III (50% formamide, 2 × SSC pH 4.5) at 65 °C. The hybridization signal of the biotin-labeled probe was first visualized using an alkaline phosphatase conjugated anti-biotin antibody (Roche) at 1 : 2000 dilution in 1% sheep serum/TBST (Tris-buffered saline, 0.1% Tween-20), and developed with HNPP (2-hydroxy-3-naphotic acid-2′-phenylanilide phosphate)/FastRed TR (4-chloro-2-methylbenzenediazonium hemi-zinc chloride salt, Roche). The sections were observed by fluorescence microscopy and photographed. The alkaline phosphatase activity of the alkaline phosphatase-conjugated anti-biotin antibody was then abolished by treatment with 100 mM glycine/HCl pH 2.2. The signal of the DIG-labeled probe was then visualized using an alkaline phosphatase-conjugated anti-DIG antibody (Roche) at 1 : 2000 dilution in the same buffer and developed with BCIP/NBT (5-bromo-4-chloro-3-indolyl-phos-

phate/nitroblue tetrazolium chloride, Roche) and photographed in the same region.

PCR

Brain RNA was extracted from 100 mg of tissue using Trizol (GibcoBRL). From 3 μg of total RNA treated with DNase I, complementary DNAs were synthesized with oligo dT primers using SuperScript II (GibcoBRL). The sequences of the 5′- and 3′-primers used for reverse transcription (RT)-PCR are as follows: 5′-CCCAAGCTTTTTCTGCTGGA-3′ and 5′-TGCCTTGTCCGTTC TTCCTG-3′, corresponding to nucleotides 903–922 and 1672–1691 of the Fez1 cDNA, respectively. GAPDH (glyceraldehyde-3-phosphate dehydrogenase) was used as an internal control. PCR was performed using AmpliTaq DNA polymerase (Perkin Elmer) with the following protocol: denaturation at 95 °C for 1 min; followed by 25 cycles of 95 °C for 20 s, 55 °C for 30 s and 72 °C for 30 s. Amplified products were analysed by electrophoresis on a 1.5% agarose gel.

Real-time quantitative RT-PCR was performed by ABI PRISM 7000 (Applied Biosystems) as described previously (Takumi *et al.*, 1999). The PCR primers were designed with Primer Express software (Applied Biosystems) and the sequences of the forward and reverse primers are as follows: 5′-CCCAGCTTCCTATCCCCATAA-3′ and 5′-TGAAGGAGAACTCGGCCTTG-3′, corresponding to nucleotides 965–985 and 1018–1037 of the Fez1 cDNA, respectively. Specificity of gene amplification was confirmed by measuring the size and purity of the PCR product by 10% acrylamide gel electrophoresis. For a 25-μL PCR reaction, 2.5 μL cDNA template was mixed with the forward and reverse primers to a final concentration of 300 nM each and 12.5 μL of 2 × SYBR Green PCR Master Mix (Applied Biosystems).

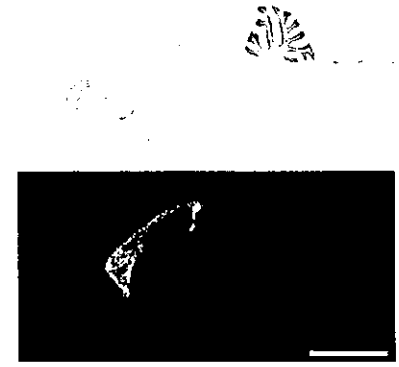

FIG. 1. Expression pattern of Fez1 in the adult mouse brain. Film autoradiographs of *in situ* hybridization on sagittal brain sections with ^{35}S-labeled probes. Upper panel shows the hematoxylin staining of the same section. Scale bar, 4 mm.

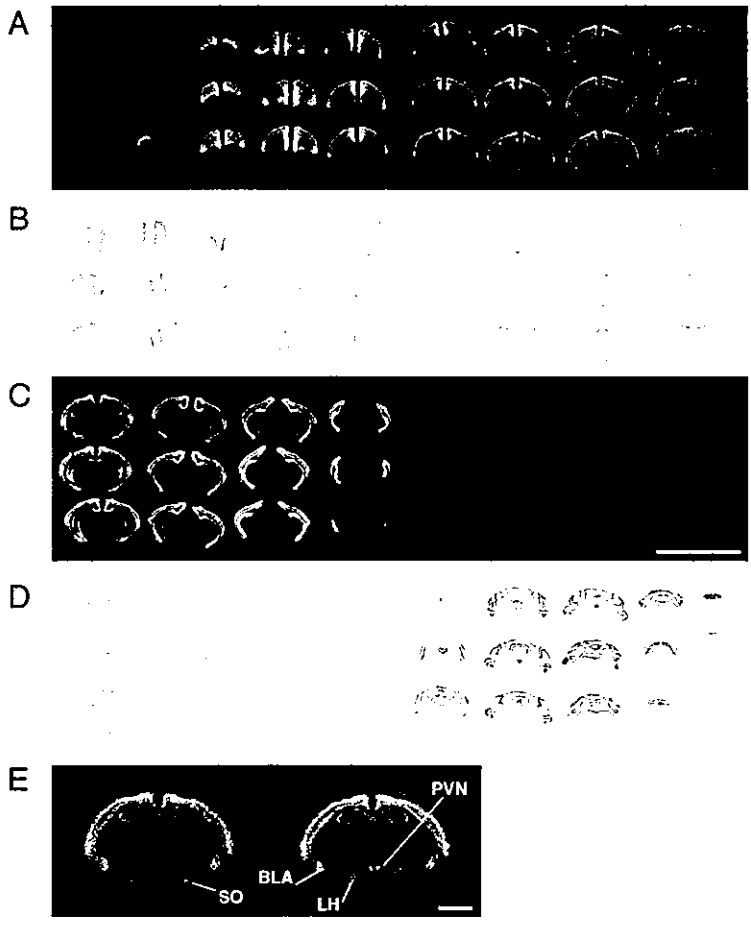

FIG. 2. Detailed expression pattern of Fez1 in the adult mouse brain. *In situ* hybridization film autoradiographs (A and C) and hematoxylin staining (B and D) of coronal sections of the adult mouse brain from the olfactory bulb to the spinal cord. A and C correspond to B and D, respectively. Expression of Fez1 mRNA in the hypothalamus and amygdala (E). BLA, basolateral amygdaloid nuclei; LH, lateral hypothalamic nuclei; PVN, paraventricular nuclei; SO, supraoptic nuclei. Scale bar, 10 mm (C) and 2 mm (E).

The reaction was first incubated at 50 °C for 2 min, then at 95 °C for 10 min, followed by 40 cycles of 95 °C for 15 s and 60 °C for 1 min. Each gene-specific PCR was performed in triplicate. GAPDH primers were used as the control.

Results

Fez1 is predominantly expressed in the adult mouse neocortex

Through systematic screening of genes specifically expressed in the adult neocortex, we identified an intriguing gene among several candidates (T. Takumi, A. Yamada and K. Inoue, unpublished data). Searching the NCBI (National Center for Biotechnology Information) database, this gene was identified as *Fez* (forebrain embryonic zinc-finger), the mouse homolog of *Xenopus* zinc-finger gene (Hashimoto *et al.*, 2000; Matsuo-Takasaki *et al.*, 2000). Fez has six C_2H_2-type zinc-finger motifs at the C-terminus and also contains a motif similar to several transcription repressors, such as Engrailed, Goosecoid, Dharma and Anf/Hes-1/Rpx1, at the N-terminus (Hashimoto *et al.*, 2000). We named the clone we identified Fez1, because we found another member in the database, called Fez2, which is very similar to Fez1 in primary amino acid, but has a different expression pattern (Takumi *et al.*, unpublished data). We first tested the subcellular localization of Fez1. Immunohistochemical analysis with an anti-Fez1 antibody showed that Fez1 proteins were localized in the nuclei of neurons in the adult neocortex (see Fig. 6J). EGFP-tagged Fez1 proteins expressed in PC12 and NIH3T3 cells were also restricted to nuclei (data not shown).

In situ hybridization clearly showed that Fez1 mRNA was strongly expressed specifically in the neocortex and subiculum and was more faintly expressed in a part of the hippocampus (CA1–3), but was not expressed in the olfactory bulb and dentate gyrus (Fig. 1). We further performed more detailed analysis of the expression pattern of Fez1 by *in situ* hybridization of many areas of the brain ranging from the olfactory bulb to the spinal cord (Fig. 2). The expression pattern of Fez1 was highly specific to the neocortex and hippocampus (CA1–3, but not the dentate gyrus), but faint expression was also seen in the supraoptic nuclei, paraventricular nuclei and lateral hypothalamic nuclei of the hypothalamus and in the basolateral nuclei of the amygdala (Fig. 2E). Furthermore, we analysed Fez1 mRNA by RT-PCR and quantified its expression using real-time RT-PCR analysis. Consistent with the *in situ* hybridization results, the expression of Fez1 was detected predominantly in the neocortex and hippocampus in representative brain regions, as well as very faintly in the hypothalamus (Fig. 3A). Fez1 mRNA was specifically detected in the brain among the different peripheral tissues of the adult mouse (Fig. 3B).

Interestingly, the specificity of Fez1 expression in the neocortex can be clearly seen by comparing its expression between the neocortex and the palaeocortex around the rhinal fissure (Fig. 4A). In contrast to its strong expression in the insular cortex of the neocortex, no Fez1 mRNA was observed in the piriform cortex of the palaeocortex. The

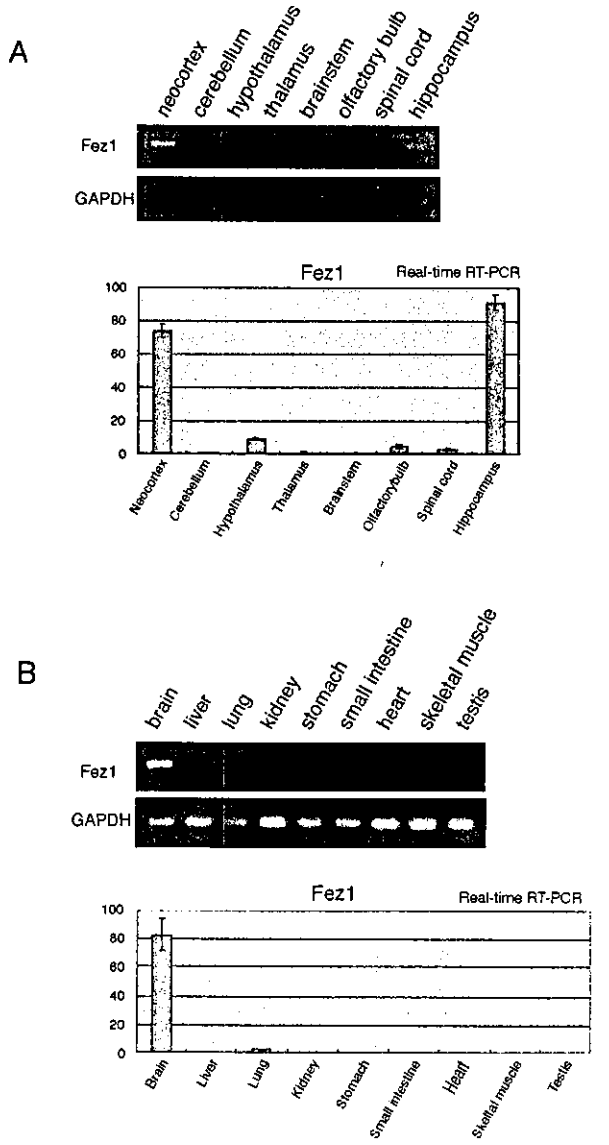

FIG. 3. Brain regional and tissue distribution pattern of Fez1 analysed by conventional reverse transcriptase-polymerase chain reaction (RT-PCR) and real-time quantitative RT-PCR. (Upper panel) mRNA expression of Fez1 and glyceraldehyde-3-phosphate dehydrogenase (GAPDH) used as an internal control in the representative brain regions (A) and tissues (B) in the adult mouse. (Lower panel) Real-time quantitative RT-PCR.

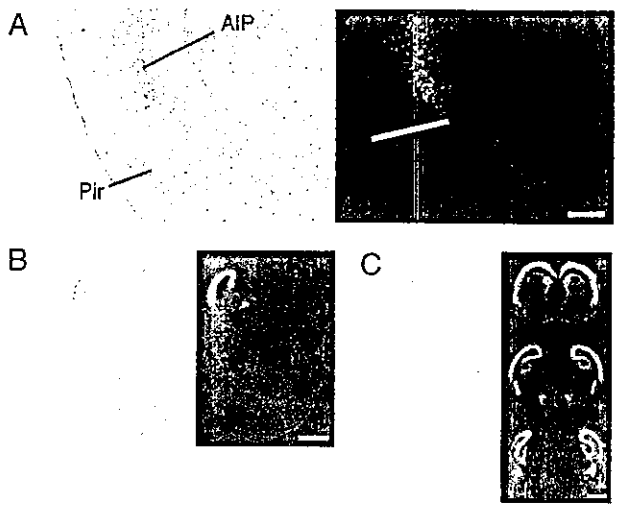

FIG. 4. (A) Fez1 mRNA expression around the rhinal fissure. AIP, agranular insular cortex; Pir, piriform cortex. A line shows the boundary between the neocortex and palaeocortex. Developmental expression of Fez1 mRNA at E14.5 (B) and P0 (C). Each left panel shows the hematoxylin staining and each right panel shows *in situ* hybridization, dark-field photomicrographs (A) and film autoradiographs (B and C), respectively. Scale bar, 300 μm (A), 2 mm (B) and 1 mm (C).

developmental expression of Fez1 mRNA was also examined by *in situ* hybridization. The expression of Fez1 mRNA in the cerebral neocortex was clearly observed at E14.5, P0 and P7 stages (Fig. 4B and C), in addition to its expression in amygdala (Fig. 4C).

Fez1 shows a deep layer-specific pattern of expression in the adult neocortex

To date several genes have been identified as being expressed specifically in the telencephalic cortex, including Emx1 (Simeone *et al.*, 1992). Some genes, including CaMKIIα, have also been identified as being forebrain specific. We compared the expression pattern of Fez1 with Emx1 and CaMKIIα in sagittal brain sections and found that Fez1 is more specifically expressed in the neocortex than these genes. Other than in the cerebral neocortex, Emx1 was strongly expressed in the olfactory bulb and the dentate gyrus, while the hybridization signal of Fez1 was very weak or absent in these areas (Fig. 5A and B). CaMKIIα expression was observed more broadly in the regions other than the cerebral cortex (Fig. 5C and F). In addition, the distribution of Fez1 in different tissues was more specific than that of Emx1. Emx1 was found to be expressed strongly in the kidney, as previously reported (Briata *et al.*, 1996), while the hybridization signal of Fez1 was only detected in the whole sagittal brain sections of the postnatal 7-day mouse (Fig. 5D and E). Moreover, Fez1 has a distinct expression pattern from that of Emx1 even in the cortex. It has been reported that Emx1 is expressed in pyramidal cells of the cortex and the hybridization signal was observed in all layers except layer I of the cortex (Chan *et al.*, 2001), whereas the hybridization signal of Fez1 was detected only in layers V and VI of the neocortex (Fig. 6A). In contrast to Fez1, Emx1 was widely expressed not only in the neocortex but also in the palaeocortex, such as in the piriform cortex.

In order to analyse the layer-specific expression of Fez1 in the adult neocortex, the expression of Fez1 was compared with that of Otx1 and SCIP. Fez1 was clearly expressed specifically in the deeper layers of neocortex, while the expression of Otx1 was very weak in the adult neocortex and that of SCIP was not specific to the deep layers but also expressed in layers II–III (Fig. 5G–I). Furthermore, immunohistochemistry using anti-Fez1 antibody showed that the immunopositive staining was localized in layers V and VI of the neocortex (Fig. 6I). Collectively these results indicate that Fez1 is expressed more specifically in the deep layers of the adult neocortex than any other genes reported so far.

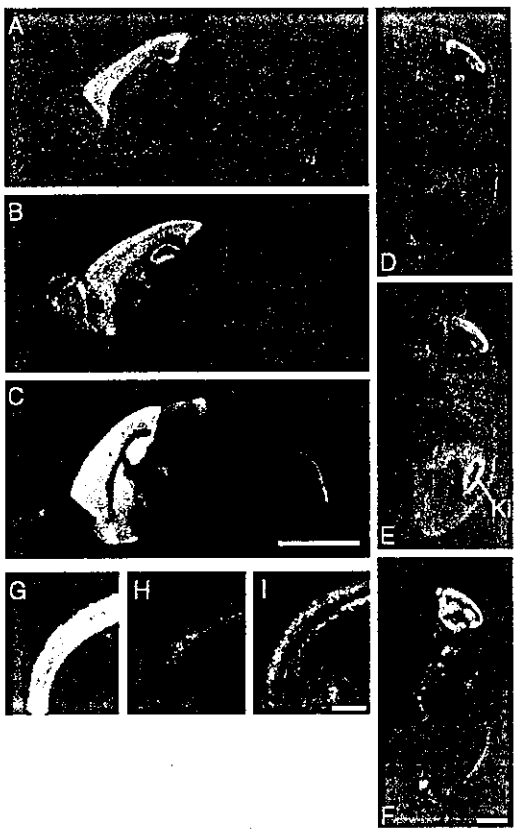

FIG. 5. Comparison of the mRNA distribution pattern of Fez1 (A, D and G), Emx1 (B and E), CaMKIIα (C and F), Otx1 (H) and SCIP (I). *In situ* hybridization film autoradiographs of sagittal (A–C) or coronal (G–I) brain sections of the adult mouse and whole sagittal sections of a postnatal day 7 mouse (D–F). Ki, kidney. Scale bar, 4 mm (A–C); 5 mm (D–F) and 1 mm (G–I).

Fez1 is expressed in glutamatergic neurons but not GABAergic neurons

We then investigated which cells in the neocortex express Fez1 by two-color double-labeling *in situ* hybridization using DIG- and biotin-labeled probes, and analysed whether Fez1 is expressed in GABAergic neurons in the neocortex. Fez1-expressing cells do not express glutamic acid decarboxylase 67 (GAD67), a marker for GABAergic neurons (Fig. 6B–D), but CaMKIIα, a marker for glutamatergic neurons (Fig. 6E–G). This, combined with morphological analysis, clearly showed that Fez1 is expressed in non-GABAergic neurons, namely in excitatory pyramidal neurons (Fig. 6B).

Fez1 expression is restricted to the deep layers of the neocortex at embryonic and postnatal stages

It has been reported that Otx1 is specifically expressed in the deep layers and the ventricular zone of the cortex during early development (Frantz *et al.*, 1994b). We compared the expression pattern of Otx1 and Fez1 in the cortex during the developmental stages (Fig. 7). In addition to the cortical layer, Otx1 was expressed strongly in the ventricular zone from the early to late embryonic stages, as reported previously (Frantz *et al.*, 1994b). Interestingly, the strong signal of Fez1 was first detected in the superficial thin layers at about E13, corresponding to the time when the cortical plate is just beginning to be constructed at the superficial layer (Fig. 7A). This expression of Fez1 in the cortical plate was detected at all embryonic stages, while no signal was detected at the ventricular and intermediate zone. At E14.5, a weak hybridization signal was detected in the subplate neurons in addition to the cortical plate. At the postnatal stages, the signal of Fez1 in neurons of the deep cortical layers remains strong, while that of Otx1 appears to weaken or disappear (Fig. 7B).

Fez1 expression in the cortex of the reeler mouse

In the neurological mutant mouse, *reeler*, a defect in the migration of cortical plate neurons prevents splitting of the preplate, resulting in a reversed laminar structure of the neocortex (Caviness, 1982). To confirm which neuronal layers express Fez1, we examined the distribution pattern of Fez1 in the adult *reeler* mouse cortex (Fig. 8). In the cerebral cortex of wild-type mouse, most Fez1-labeled cells in layer V were strongly labeled, whereas most labeled cells in layer VI are weakly labeled (Fig. 8A and B). In the cerebral cortex of the *reeler*

FIG. 6. Cellular distribution of Fez1 mRNA in the adult mouse brain. (A) *In situ* hybridization emulsion autoradiograph of a ^{35}S-labeled Fez1 probe in the neocortex performed on coronal brain sections of the adult mouse. (B) *In situ* hybridization signal of a DIG-labeled Fez1 probe in layer V of the cerebral neocortex in a sagittal brain section of the adult mouse. Arrows indicate cells with the typical soma shape of pyramidal cells. (C and D) Two-color double-labeling *in situ* hybridization with a biotin-labeled GAD67 probe or CaMKIIα and DIG-labeled Fez1 probe. Hybridization signals were visualized with HNPP/FastRed TR for the biotin-labeled GAD67 probe (C) or CaMKIIα (F), and with BCIP/NBT for the DIG-labeled Fez1 probe (D and G). (E and H) Overlay of the images shown in C and F, and D and G. Immunohistochemical staining of the mouse cortex with Fez1 antibody (I and J). Scale bar, 100 μm (A), 25 μm (B), 50 μm (C–H), 200 μm (I) and 50 μm (J).

mouse, on the other hand, strongly labeled cells were scattered widely throughout all layers of the cortex, whereas weakly labeled cells were mainly distributed just beneath the pial surface (Fig. 8C and D). This distribution pattern is very similar to the pattern of retrograde labeled cells after injection of dye into the spinal cord and thalamus of adult wild-type and *reeler* mice (Yamamoto *et al.*, 2003).

Discussion

The mammalian neocortex, which contains over 10 billion neurons in humans, is an associative center of our sensory, motor and cognitive functions. Recent studies using molecular biology and genetics have identified various genes involved in brain development, but even now that the human genome sequence is available, our understanding of the adult neocortex at the molecular level is still at a primitive stage despite its functional importance. Using a global screening approach, we identified Fez1 as a gene predominantly expressed in the adult mouse neocortex. Fez1 will be valuable not only for exploring the developmental contribution or physiological function of the adult neocortex, but also for using its promoter in gene-manipulated animals. A promoter that controls the expression of a transgene specifically in the neocortex could be used for conditional strategies.

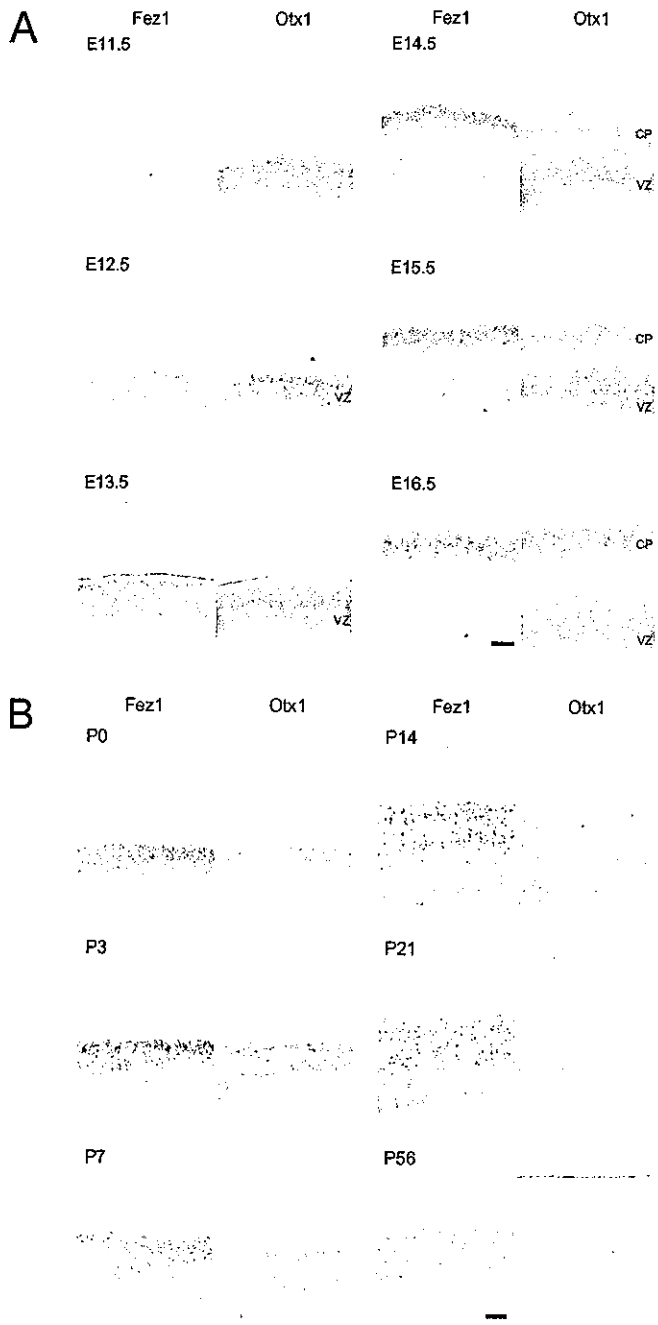

FIG. 7. Fez1 and Otx1 mRNA expression in the cortex during prenatal (A) and postnatal (B) stages. Hybridization signals of the DIG-labeled probes were visualized with BCIP/NBT (purple). Prenatal sections were counterstained with eosin (pink). CP, cortical plate; VZ, ventricular zone. Scale bar, 100 μm (A) and 200 μm (B).

Cerebral cortex-specific promoters

As described above, through systematic screening, we identified Fez1, a gene expressed primarily in the neocortex, and not in the palaeocortex. Up to date, the promoters of Emx1 and CaMKIIα have been used for regulating gene expression in the adult cerebral cortex (Tsien *et al.*, 1996; Iwasato *et al.*, 2000). However, regional specificity of these two genes is lower than that of Fez1. Besides the neocortex, our results showed that Emx1 is strongly expressed in the olfactory bulb and the hippocampus and weakly expressed in the brainstem.

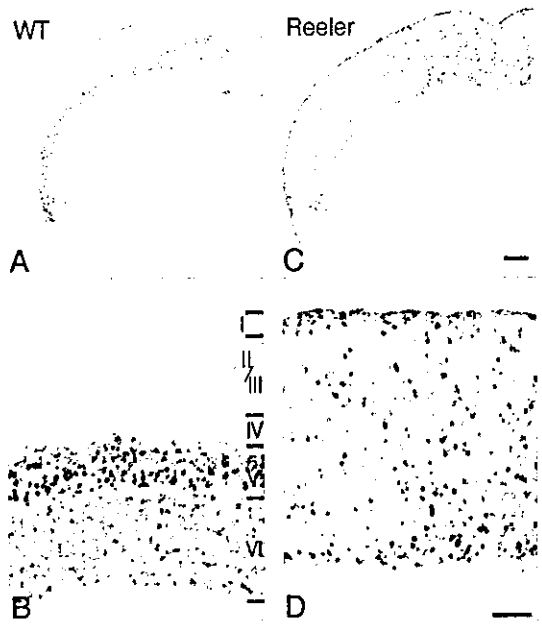

FIG. 8. mRNA expression pattern of Fez1 in the adult wild-type and *reeler* mouse cortex. Upper panels show *in situ* hybridization signals of the DIG-labeled Fez1 probe in coronal wild-type (A) and *reeler* (C) mouse brain sections. The lower panels show high-magnification views of wild-type (B) and *reeler* (D) sections. Scale bar, 500 μm (A and C) and 200 μm (B and D).

Furthermore, strong expression was also observed in the kidney. The specificity of CaMKIIα expression was even lower than that of Emx1. CaMKIIα was strongly expressed in the hippocampus and striatum, and a weak to intermediate level of expression was observed in the olfactory bulb, septum, thalamus, inferior colliculus, spinal cord and Purkinje cells in the cerebellum (Erondu & Kennedy, 1985; Burgin *et al.*, 1990). Therefore, the use of the Fez1 promoter would be more beneficial for neocortex-specific gene manipulation in adult mice.

It has been reported that Fez1 is also expressed in the ventral forebrain during the embryonic stages of the zebrafish and mouse (Hashimoto *et al.*, 2000; Matsuo-Takasaki *et al.*, 2000). Furthermore, it has been shown that mutation of zebrafish Fez leads to loss of diencephalic monoaminergic neurons in a non-cell-autonomous manner (Levkowitz *et al.*, 2003). Our results showed that Fez1 is also expressed in the embryonic hypothalamus. However, this expression in the hypothalamus was reduced in the postnatal mouse brain and only a faint signal was observed in the adult hypothalamus, whereas the strong expression of Fez1 in the neocortex is maintained into adulthood. Therefore, the different expression pattern of Fez1 in the hypothalamus and neocortex indicates that Fez1 may play distinct roles in brain development and maintenance of adult brain functions.

A marker for pyramidal cells of the cerebral neocortex in layers V and VI

The Fez family is highly conserved among many species from worms to humans. In zebrafish and *Xenopus*, Fez is expressed mainly in the forebrain and is thought to play a role in forebrain development (Hashimoto *et al.*, 2000; Matsuo-Takasaki *et al.*, 2000). In zebrafish, Fez is reported to induce *dlx2* and *dlx6* expression (Yang *et al.*, 2001). These homeobox genes are also highly conserved between species and are involved in the development of the brain. Recently, Dlx genes were reported to induce GADs in slice cultures of the mouse embryonic cerebral cortex (Stuhmer *et al.*, 2002). These reports imply that Fez may regulate GABAergic specification through regulation of Dlx expression. However, our results showed that Fez1 is not expressed in GABAergic neurons but in pyramidal cells, at least in some populations of the adult mouse cerebral neocortex.

The vertebrate cerebral neocortex is organized into six layers (I–VI). Each layer shows a characteristic feature of the constituent cell type, density and axonal connections. Although the pyramidal cells are present in layers II–VI, Fez1 is specifically expressed in layers V and VI of the adult mouse cerebral neocortex. Layers V and VI contain pyramidal cells that project their axons to the subcortical areas, whereas pyramidal cells of the superficial layers send their axons to other cortical areas. Several genes have been reported to show layer-specific patterns of expression (Hevner *et al.*, 2003). Genes reported to be specifically expressed in layers V–VI of neocortex include the POUIII domain transcription factor SCIP/Oct-6/tst-1 (He *et al.*, 1989; Frantz *et al.*, 1994a), the homeodomain protein Otx1 (Frantz *et al.*, 1994b), the ETS transcription factor er81 (Weimann *et al.*, 1999) and the receptor-like protein-tyrosine phosphatase PTPλ (Cheng *et al.*, 1997). SCIP/Oct-6/tst-1 is a multifunctional transcription factor, and its involvement in peripheral myelination (Jaegle *et al.*, 1996) and differentiation of the epidermis (Andersen *et al.*, 1997) are well characterized; however, its contribution to neural development in the CNS remains to be elucidated. Analysis of Otx1 mutant mice revealed that Otx1 is required for the refinement of exuberant axonal projections of cortical efferent neurons (Weimann *et al.*, 1999). Er81 has been reported to regulate the development of selective connections between sensory and motor neurons in the spinal cord as well as to be involved in carcinogenesis (Arber *et al.*, 2000; Goel & Janknecht, 2003). A comparison of these molecular markers including Fez1 identified here is as follows. All genes described above are expressed in the forebrain from the early stages of corticogenesis. However, among them, Otx1 expression in the neocortex is dramatically reduced in the adult mouse. The expression of SCIP/Oct-6/tst-1 in the adult neocortex is seen in layers II–III in addition to layers V–VI, and it is also expressed in a variety of brain regions in the adult, such as the CA1 area of the hippocampus, subiculum, striatum, tenia tecta and indusium griseum, the peripheral nervous system (PNS) and even in the testis (He *et al.*, 1989; Frantz *et al.*, 1994a). Er81 is expressed in the spinal cord and PNS, as well as various peripheral tissues including kidney, heart and lung (Brown & McKnight, 1992; Arber *et al.*, 2000). PTPλ expression in the adult brain appears to be downregulated, and other areas of prominent expression include the piriform cortex, endopiriform nucleus, amygdaloid nuclei, subiculum, and CA1 and CA2 of the hippocampal formation as well as peripheral tissues such as lung and kidney (Cheng *et al.*, 1997). Thus, Fez1 may serve as an ideal molecular marker that is specifically expressed in layers V–VI of the adult neocortex. Furthermore, the expression of Fez1 in adults suggests that it is necessary not only for the establishment but also for the maintenance of layer-related cell fates.

In the *reeler* mouse, Fez1-positive neurons, which are confined to the deep layers of the normal neocortex, are radially intermingled in the adult neocortex (Fig. 8). This distribution pattern of Fez1-positive neurons is very similar to that of corticospinal tract (CST) and corticothalamic tract (CTT) neurons identified by retrograde labeling (Yamamoto *et al.*, 2003). Strongly labeled neurons that are likely to be CST neurons were located in layer V of wild-type mouse and were widely scattered throughout all depths of the cortex in the *reeler* mouse, while weakly labeled neurons that are likely to be CTT neurons were expressed in layer VI of wild-type mouse and were mainly distributed just beneath the pia mater in the *reeler* mouse. Moreover, as observed in

the wild-type mouse cortex, the hybridization signal in the insular cortex was stronger than the other areas of the cortex of the *reeler* mouse, suggesting that tangential organization is not impaired in the *reeler* mouse (Fig. 8). These data suggest that Fezl is expressed at least in CTT and CST neurons even in the *reeler* mouse. Combined with the finding that Fezl is induced in these neurons before they extend their axons to the subcortical areas at E13.5 (Fig. 7), this observation suggests that Fezl might play a role in axonal outgrowth and targeting to these areas. In fact, our preliminary results of experiments using knockout mice of the Fez family are compatible with this possibility. Further detailed examination will uncover the function of Fezl in the cerebral cortex.

Acknowledgements

We thank Hiroyuki Aburatani, Masami Ishii, Asami Umino, Kumiko Hamajima, Atsuko Yamada, Yoko Sakakida, Setsuko Tsuboi and Chiaki Matsubara for their technical assistance, and Takahisa Furukawa for suggestions with *in situ* hybridization. We also thank Masahiko Hibi for sharing their unpublished information, and Paul Burke and Dan Trcka for reviewing the manuscript. This work was supported in part by research grants from MEXT, the Ichiro Kanehara Foundation, Mitsubishi Pharma Research Foundation and Sony Corporation.

Abbreviations

CaMKIIα, alpha subunit of the calcium/calmodulin-dependent protein kinase II; CST, corticospinal tract; CTT, corticothalamic tract; DIG, digoxigenin; GABA, γ-aminobutyric acid; GAD67, glutamic acid decarboxylase 67; GAPDH, glyceraldehyde-3-phosphate dehydrogenase; HNPP, 2-hydroxy-3-naphotic acid-2′-phenylanilide phosphate; NBT, nitroblue tetrazolium chloride; PB, phosphate buffer; PCR, polymerase chain reaction; RT, reverse transcriptase; SSC, standard sodium citrate.

References

Andersen, B., Weinberg, W.C., Rennekampff, O., Mcevilly, R.J., Bermingham, J.R. Jr, Hooshmand, F., Vasilyev, V., Hansbrough, J.F., Pittelkow, M.R., Yuspa, S.H. & Rosenfeld, M.G. (1997) Functions of the POU domain genes Skn-1a/i and Tst-1/Oct-6/SCIP in epidermal differentiation. *Genes Dev.*, **11**, 1873–1884.

Arber, S., Ladle, D.R., Lin, J.H., Frank, E. & Jessell, T.M. (2000) ETS gene Er81 controls the formation of functional connections between group Ia sensory afferents and motor neurons. *Cell*, **101**, 485–498.

Briata, P., Di Blas, E., Gulisano, M., Mallamaci, A., Iannone, R., Boncinelli, E. & Corte, G. (1996) EMX1 homeoprotein is expressed in cell nuclei of the developing cerebral cortex and in the axons of the olfactory sensory neurons. *Mech. Dev.*, **57**, 169–180.

Brown, T.A. & Mcknight, S.L. (1992) Specificities of protein–protein and protein–DNA interaction of GABP alpha and two newly defined ets-related proteins. *Genes Dev.*, **6**, 2502–2512.

Burgin, K.E., Waxham, M.N., Rickling, S., Westgate, S.A., Mobley, W.C. & Kelly, P.T. (1990) In situ hybridization histochemistry of Ca2+/calmodulin-dependent protein kinase in developing rat brain. *J. Neurosci.*, **10**, 1788–1798.

Caviness, V.S. Jr (1982) Neocortical histogenesis in normal and reeler mice: a developmental study based upon [3H]thymidine autoradiography. *Brain Res.*, **256**, 293–302.

Chan, C.H., Godinho, L.N., Thomaidou, D., Tan, S.S., Gulisano, M. & Parnavelas, J.G. (2001) Emx1 is a marker for pyramidal neurons of the cerebral cortex. *Cereb. Cortex*, **11**, 1191–1198.

Cheng, J., Wu, K., Armanini, M., O'Rourke, N., Dowbenko, D. & Lasky, L.A. (1997) A novel protein-tyrosine phosphatase related to the homotypically adhering kappa and mu receptors. *J. Biol. Chem.*, **272**, 7264–7277.

Chenn, A., Braisted, J.E., McConnell, S.K. & O'Leary, D.D.M. (1997) Development of the cerebral cortex: mechanisms controlling cell fate, laminar and areal patterning, and axonal connectivity. In Cowan, W.M., Jessell, T.M. & Zipursky, S.L. (Eds), *Molecular and Cellular Approaches to Neural Development*. Oxford University Press, New York, pp. 440–473.

Erondu, N.E. & Kennedy, M.B. (1985) Regional distribution of type II Ca2+/calmodulin-dependent protein kinase in rat brain. *J. Neurosci.*, **5**, 3270–3277.

Frantz, G.D., Bohner, A.P., Akers, R.M. & McConnell, S.K. (1994a) Regulation of the POU domain gene SCIP during cerebral cortical development. *J. Neurosci.*, **14**, 472–485.

Frantz, G.D., Weimann, J.M., Levin, M.E. & McConnell, S.K. (1994b) Otx1 and Otx2 define layers and regions in developing cerebral cortex and cerebellum. *J. Neurosci.*, **14**, 5725–5740.

Garel, S., Huffman, K.J. & Rubenstein, J.L. (2003) Molecular regionalization of the neocortex is disrupted in Fgf8 hypomorphic mutants. *Development*, **130**, 1903–1914.

Goel, A. & Janknecht, R. (2003) Acetylation-mediated transcriptional activation of the ETS protein ER81 by p300, P/CAF, and HER2/Neu. *Mol. Cell. Biol.*, **23**, 6243–6254.

Grove, E.A. & Fukuchi-Shimogori, T. (2003) Generating the cerebral cortical area map. *Annu. Rev. Neurosci.*, **26**, 355–380.

Hashimoto, H., Yabe, T., Hirata, T., Shimizu, T., Bae, Y., Yamanaka, Y., Hirano, T. & Hibi, M. (2000) Expression of the zinc finger gene fez-like in zebrafish forebrain. *Mech. Dev.*, **97**, 191–195.

He, X., Treacy, M.N., Simmons, D.M., Ingraham, H.A., Swanson, L.W. & Rosenfeld, M.G. (1989) Expression of a large family of POU-domain regulatory genes in mammalian brain development. *Nature*, **340**, 35–41.

Hevner, R.F., Daza, R.A., Rubenstein, J.L., Stunnenberg, H., Olavarria, J.F. & Englund, C. (2003) Beyond laminar fate: toward a molecular classification of cortical projection/pyramidal neurons. *Dev. Neurosci.*, **25**, 139–151.

Iwasato, T., Datwani, A., Wolf, A.M., Nishiyama, H., Taguchi, Y., Tonegawa, S., Knopfel, T., Erzurumlu, R.S. & Itohara, S. (2000) Cortex-restricted disruption of NMDAR1 impairs neuronal patterns in the barrel cortex. *Nature*, **406**, 726–731.

Jaegle, M., Mandemakers, W., Broos, L., Zwart, R., Karis, A., Visser, P., Grosveld, F. & Meijer, D. (1996) The POU factor Oct-6 and Schwann cell differentiation. *Science*, **273**, 507–510.

Kandel, E.R., Schwartz, J.H. & Jessell, T.M. (2000) *Principles of Neural Science*. McGraw-Hill, New York.

Levkowitz, G., Zeller, J., Sirotkin, H.I., French, D., Schilbach, S., Hashimoto, H., Hibi, M., Talbot, W.S. & Rosenthal, A. (2003) Zinc finger protein too few controls the development of monoaminergic neurons. *Nat. Neurosci.*, **6**, 28–33.

Matsuo-Takasaki, M., Lim, J.H., Beanan, M.J., Sato, S.M. & Sargent, T.D. (2000) Cloning and expression of a novel zinc finger gene, Fez, transcribed in the forebrain of Xenopus and mouse embryos. *Mech. Dev.*, **93**, 201–204.

Muzio, L., Dibenedetto, B., Stoykova, A., Boncinelli, E., Gruss, P. & Mallamaci, A. (2002) Conversion of cerebral cortex into basal ganglia in Emx2 (-/-) Pax6 (Sey/Sey) double-mutant mice. *Nat. Neurosci.*, **5**, 737–745.

O'Leary, D.D. (1989) Do cortical areas emerge from a protocortex? *Trends Neurosci.*, **12**, 400–406.

O'Leary, D.D. & Nakagawa, Y. (2002) Patterning centers, regulatory genes and extrinsic mechanisms controlling arealization of the neocortex. *Curr. Opin. Neurobiol.*, **12**, 14–25.

Rakic, P. (1988) Specification of cerebral cortical areas. *Science*, **241**, 170–176.

The RIKEN Genome Exploration Research Group Phase II Team and the FANTOM Consortium (2001) Functional annotation of a full-length mouse cDNA collection. *Nature*, **409**, 685–690.

Simeone, A., Gulisano, M., Acampora, D., Stornaiuolo, A., Rambaldi, M. & Boncinelli, E. (1992) Two vertebrate homeobox genes related to the Drosophila empty spiracles gene are expressed in the embryonic cerebral cortex. *EMBO J.*, **11**, 2541–2550.

Stuhmer, T., Anderson, S.A., Ekker, M. & Rubenstein, J.L. (2002) Ectopic expression of the Dlx genes induces glutamic acid decarboxylase and Dlx expression. *Development*, **129**, 245–252.

Takumi, T., Nagamine, Y., Miyake, S., Matsubara, C., Taguchi, K., Takekida, S., Sakakida, Y., Nishikawa, K., Kishimoto, T., Niwa, S., Okumura, K. & Okamura, H. (1999) A mammalian ortholog of Drosophila timeless, highly expressed in SCN and retina, forms a complex with mPER1. *Genes Cells*, **4**, 67–75.

Tsien, J.Z., Chen, D.F., Gerber, D., Tom, C., Mercer, E.H., Anderson, D.J., Mayford, M., Kandel, E.R. & Tonegawa, S. (1996) Subregion- and cell type-restricted gene knockout in mouse brain. *Cell*, **87**, 1317–1326.

Weimann, J.M., Zhang, Y.A., Levin, M.E., Devine, W.P., Brulet, P. & McConnell, S.K. (1999) Cortical neurons require Otx1 for the refinement of exuberant axonal projections to subcortical targets. *Neuron*, **24**, 819–831.

Yamamoto, T., Sakakibara, S., Mikoshiba, K. & Terashima, T. (2003) Ectopic corticospinal tract and corticothalamic tract neurons in the cerebral cortex of yotari and reeler mice. *J. Comp. Neurol.*, **461**, 61–75.

Yang, Z., Liu, N. & Lin, S. (2001) A zebrafish forebrain-specific zinc finger gene can induce ectopic dlx2 and dlx6 expression. *Dev. Biol.*, **231**, 138–148.

Journal of Neurochemistry, 2004, **90**, 1378–1388 doi:10.1111/j.1471-4159.2004.02592.x

Effects of psychotomimetic and antipsychotic agents on neocortical and striatal concentrations of various amino acids in the rat

Shin-ichiro Sakurai, Sumikazu Ishii, Asami Umino, Dai Shimazu, Naoki Yamamoto and Toru Nishikawa

Psychiatry and Behavioral Sciences, Tokyo Medical and Dental University Graduate School, Tokyo, Japan

Abstract

A subcutaneous injection of small and moderate doses (1.6, 3.2, 4.0 and 4.8 mg/kg) of the schizophrenomimetic methamphetamine caused a dose-related increase in the tissue content (the net content) of L-Arg and L-Asn in the neocortex and striatum at 60 min, but not at 360 min, after injection. The methamphetamine-induced (4.8 mg/kg) increases in levels of these amino acids were significantly attenuated by pretreatment with an antipsychotic drug, haloperidol (1 mg/kg) or clozapine (10 mg/kg). In the neocortex, a clozapine-reversible increase in the level of L-Thr was also observed 60 min after methamphetamine administration. Striatal concentrations of L-Glu, L-Ser, L-Thr, Gly and L-Ala were augmented by the same regimen in a haloperidol- and clozapine-sensitive fashion. A moderate dose of another schizophrenomimetic phencyclidine (7.5 mg/kg) given subcutaneously induced robust abnormal behavior, a diminution in the neocortical and striatal levels of L-Asp and an increase in the striatal L-Ala content without significant effects on the other amino acids studied. These results suggest that neocortical and striatal L-Arg, L-Asn, L-Thr, Gly, L-Ala or L-Ser may be implicated in the psychotomimetic effects of methamphetamine and might display mutual interaction with cerebral dopaminergic transmission. The differential effects of methamphetamine and phencyclidine on the net neocortical and striatal concentrations of various amino acids might, at least in part, underlie the distinct features of psychoses induced by these two drugs.

Keywords: antipsychotics, L-arginine, L-asparagine, metamphetamine, neocortex, striatum.

J. Neurochem. (2004) **90**, 1378–1388.

Intrinsic amino acids in the mammalian brain have been found to play a variety of crucial roles in excitatory and inhibitory neurotransmission and their modulation. It is well established that Glu and Asp cause an excitatory postsynaptic potential of the neuronal membrane (Hollmann and Heinemann 1994), whereas GABA, Gly and taurine (Tau) induce an inhibitory postsynaptic potential (Huxtable 1992; Olsen 2002). More recently, D-Ser and Gly have been shown to act as co-agonists for the NMDA-type excitatory amino acid receptor (Danysz and Parsons 1998).

These amino acids appear to be involved in the regulation and pathophysiology of higher brain functions such as cognition, thought, emotion and perception in humans. Thus, agonists for the benzodiazepine site of the $GABA_A$ receptor ameliorate anxiety and panic attack (Biggio *et al.* 1995; Olsen 2002). Inverse agonists for this site, in turn, cause or augment anxiety (Braestrup *et al.* 1982; Bonetti *et al.* 1988). Interruption of NMDA receptor-mediated neurotransmission results in memory disturbance, schizophrenia-like psychosis or cerebellar ataxia (Javitt 2002; Tanii *et al.* 1994; Ogawa *et al.* 2003). In support of these observations, the facilitation of excitatory signaling by Gly, D-Ser or D-cycloserine has been reported to improve schizophrenic symptoms (Contreras 1990; Tanii *et al.* 1991, 1994; Hashimoto *et al.* 1991; Javitt 2002) or ataxia in patients with spino-cerebellar degeneration (Ogawa *et al.* 2003). Moreover, altered indices of GABA and Glu systems, including tissue concentrations (which are defined as 'net concentrations' in this study), and binding, release and uptake activities have been found in the CSF,

Received January 28, 2004; revised manuscript received May 9, 2004; accepted May 11, 2004.

Address correspondence and reprint requests to T. Nishikawa, Psychiatry and Behavioral Sciences, Tokyo Medical and Dental University Graduate School, 1-5-45, Bunkyo-ku, Yushima, Tokyo 113–8519, Japan. E-mail: tnis.psyc@tmd.ac.jp

Abbreviations used: CLZ, clozapine; HAL, haloperidol; MAP, methamphetamine; NO, nitric oxide; PCP, phencyclidine.

blood, post-mortem brain tissues or by brain imaging of neuropsychiatric patients and in animal models of neuropsychiatric disorders (Carlsson *et al.* 2001). However, there are only a few reports of a systematic approach to the possible pathogenetic or pathophysiological roles of various amino acids in brain dysfunction (Kubota *et al.* 2002).

In the present study, to obtain an insight into the hypothetical disturbance of NMDA receptor function in schizophrenia and the unknown target systems for schizophrenomimetic and antipsychotic drugs, we have studied the effects of these psychotropic agents on the net content of rat neocortical and striatal amino acids that are postulated to participate directly or indirectly in control of the excitatory amino acid receptor. To this end, we have quantified three groups of amino acids: (1) excitatory amino acids acting at the Glu site of the NMDA receptor and their potential metabolites (L-Glu, L-Gln, L-Asp and L-Asn) (Reubi *et al.* 1980; Hollmann and Heinemann 1994; Dieterich *et al.* 2003; Waagepetersen *et al.* 2003); (2) amino acids acting at the co-agonist (Gly) site of the NMDA receptor (Gly and D-Ser) (Danysz and Parsons 1998) and L-Ser, a potential precursor for these NMDA co-agonists (Takahashi *et al.* 1997); and (3) a precursor of nitric oxide (NO), a diffusible gas regulator of the NMDA receptor, L-Arg (Kuriyama and Ohkuma 1995). The net concentrations of Tau, a putative inhibitory neurotransmitter, and L-Thr and L-Ala, neutral amino acids with undefined effects on neural activity, have also been measured in the two brain areas for comparison because interactions between these amino acids and psychotropic drugs are largely unknown.

For these pharmacological experiments, we have chosen different types of schizophrenia-related drugs: dopaminergic psychotomimetic methamphetamine (MAP) (Nishikawa *et al.* 1983; Seiden *et al.* 1993), glutamatergic psychotomimetic phencyclidine (PCP) (Tanii *et al.* 1994; Javitt 2002) as a comparison, typical antipsychotic haloperidol (HAL) and atypical antipsychotic clozapine (CLZ) (Miyamoto *et al.* 2002). The neocortex and striatum were selected for this quantitative examination, because some neocortico-striatal pathways have been shown to be involved in the pathophysiology of psychotogen-induced abnormal behavior (Hashimoto *et al.* 1998) and of schizophrenia (Carlsson *et al.* 2001; Tekin and Cummings 2002).

Materials and methods

Animals

The present animal experiments were performed in strict accordance with the guidance of the Tokyo Medical and Dental University and were approved by the Animal Investigation Committee of the Institution. Male Wistar rats (ST strain; Clea Japan, Inc., Tokyo, Japan) at postnatal day 56, weighing 200–230 g, were used. The animals were housed at 22.0 ± 0.5°C in a humidity-controlled room under a 12-h light–dark cycle and had free access to food and water.

Chemicals

PCP hydrochloride was kindly synthesized and donated by Yamanouchi Pharmaceutical, Co., Ltd. (Tsukuba, Japan). MAP hydrochloride was purchased from Dainippon Pharmaceutical Co., Ltd. (Osaka, Japan) with official permission of the Tokyo Metropolitan Bureau of Public Health. The other chemicals used were of ultrapure quality and commercially available.

Drug administration

MAP hydrochloride and PCP hydrochloride were dissolved in physiological saline for subcutaneous (s.c.) injection. HAL and CLZ were dissolved in 0.15% tartaric acid (Kusumi *et al.* 1995) and titrated with 0.05 M NaOH to approximately pH 5.0. HAL, CPZ and vehicle (0.15% tartaric acid, titrated as above) were administered intraperitoneally (i.p.). All injections were made immediately before administration at a volume of 1.0 mL/kg. Some animals were pretreated with HAL (1.0 mg/kg) or CLZ (10.0 mg/kg) 30 min before MAP (4.8 mg/kg) administration. Control animals were injected with saline or the vehicle instead.

Doses always refer to the free bases and were selected for the following reasons: (1) the smaller dose 1.6 mg/kg and larger doses 4.0 and 4.8 mg/kg of MAP induce different behavioral changes, hyperlocomotion and stereotypy respectively (Nishikawa *et al.* 1983); (2) PCP at 7.5 mg/kg causes robust hyperactivity, stereotyped behavior and ataxia (Tanii *et al.* 1994); (3) 1.0 mg/kg HAL completely blocks the behavioral effects of the larger doses of MAP (Ujike *et al.* 1988; Shirayama *et al.* 2000); and (4) 10.0 mg/kg CLZ is generally accepted to show the pharmacological properties as an atypical antipsychotic in animal models of schizophrenia (e.g. anti-PCP effects) (Qiao *et al.* 2001; Sams-Dodd 1996). The effects of MAP, HAL and CLZ on various amino acids in the brain were examined at 60 min and also 360 min after their administration because changes in neocortical D-Ser levels have been found to peak at 360 min after systemic administration of Gly or L-Ser (Takahashi *et al.* 1997).

Tissue preparation

Rats were killed by cervical dislocation 60 or 360 min after acute injection of MAP or PCP. According to the atlas of Paxinos and Watson 1986), the neocortex (the dorsal part of the cerebral cortex divided along the rhinal fissure) and striatum were rapidly removed in the cold, frozen in liquid nitrogen, and stored at − 80°C until use.

HPLC analysis of amino acids

The simultaneous determination of amino acid enantiomers and non-chiral amino acids in the human cortex was accomplished by HPLC with fluorometric detection as described previously but with minor modifications (Hashimoto *et al.* 1992b). Briefly, the brain sample was homogenized in 10 volumes of 4% trichloroacetic acid after the addition of D-homocysteic acid, and the homogenate was centrifuged at 14 500 *g* for 20 min at 4°C. The supernatant was stored at − 80°C until derivatization. The resulting sample was derivatized with *N-tert*-butyloxycarbonyl-L-cystein and *o*-phthaldialdehyde for 2 min at room temperature. The amino acid derivative was immediately applied to the HPLC system and separated on a

4-μm Nova-Pak C18 column (300 × 3.9 mm internal diameter; Waters, Tokyo, Japan). The column was operated at a constant flow rate of 0.9 mL/min at 30°C. Mobile phase A was 0.1 M acetate buffer (pH 6.0) containing 12% acetonitrile; mobile phase B was 0.1 M acetate buffer containing 20% acetonitrile. The separation of amino acid derivatives was performed with a linear gradient from mobile phase A to B in 50 min. Fluorescent amino acid derivatives were detected in an FP-2025 spectrofluorometer (Jasco International Co. Ltd, Tokyo, Japan). Excitation and emission wavelengths were 344 and 443 nm respectively. The reliability of the quantitative analysis for D-, L- and non-chiral amino acids was established by comparing its result with those obtained by gas chromatography (GC) or GC–mass spectrometric assay methods (Hashimoto *et al.* 1992a,b).

Statistical analysis

The statistical significance of the data was evaluated using one-way ANOVA followed by the Scheffé post-hoc test for the quantitative analysis of the amino acid concentrations.

Results

Effects of acute injection of MAP, PCP, HAL and CLZ on the net content of various amino acids in rat neocortex and striatum at 60 min after injection

In the neocortex, acute administration of MAP (1.6, 3.2 or 4.0 mg/kg, s.c.) caused a dose-related and marked increase in

Table 1 Effects of acute injection of psychostimulant or antipsychotic on the net concentrations of various amino acids in the rat neocortex at 60 min post-injection

	Amino acid concentration (μmol/g of wet weight)				
	NMDA receptor-related amino acids				
	Glutamate site				Nitric oxide
Injection (mg/kg, s.c. or i.p.)	L-Glu	L-Gln	L-Asp	L-Asn	L-Arg
Saline	13.6±0.1	5.06±0.06	3.96±0.08	0.113±0.002	0.090±0.002
MAP (1.6)	14.5±0.1	4.90±0.07	3.51±0.03*	0.118±0.002	0.115±0.006*
MAP (3.2)	14.8±0.2*	4.96±0.07	3.60±0.09	0.159±0.010**	0.129±0.011**
MAP (4.0)	14.2±0.4	4.68±0.11*	4.02±0.09	0.172±0.005**	0.163±0.007**
PCP (7.5)	14.1±0.3	5.22±0.08	3.57±0.04*	0.115±0.003	0.099±0.003
HAL (1.0)	12.8±0.5	5.28±0.12	4.26±0.14	0.114±0.002	0.087±0.003
CLZ (10.0)	12.9±0.2	5.22±0.13	4.30±0.04	0.108±0.004	0.080±0.004

	Amino acid concentration (μmol/g of wet weight)					
	NMDA receptor-related amino acids					
	Glycine site			Other amino acids		
Injection (mg/kg, s.c. or i.p.)	Gly	D-Ser	L-Ser	Tau	L-Thr	L-Ala
Saline	0.94±0.02	0.251±0.002	1.05±0.02	5.71±0.07	0.599±0.008	0.685±0.010
MAP (1.6)	0.94±0.02	0.263±0.003	1.00±0.02	5.76±0.06	0.612±0.017	0.712±0.005
MAP (3.2)	1.01±0.03	0.251±0.003	1.09±0.03	5.64±0.05	0.627±0.021	0.787±0.010**
MAP (4.0)	1.08±0.03**	0.255±0.002	1.22±0.03**	5.68±0.06	0.722±0.018**	0.734±0.017
PCP (7.5)	0.94±0.03	0.250±0.002	0.99±0.01	5.62±0.08	0.632±0.009	0.732±0.019
HAL (1.0)	0.95±0.01	0.258±0.002	1.06±0.01	5.81±0.04	0.604±0.020	0.650±0.004
CLZ (10.0)	0.94±0.02	0.255±0.003	1.04±0.01	5.84±0.08	0.588±0.012	0.663±0.011

Rats were treated with a subcutaneous injection of saline, MAP or PCP, or an intraperitoneal injection of HAL or CLZ acutely, and were killed 60 min thereafter. The amino acids quantified in this study are divided into the following four groups that are defined in view of the relations to the NMDA receptor: (1) excitatory amino acids acting at the glutamate site of the NMDA receptor and their potential metabolites, L-glutamate, L-glutamine, L-aspartate, L-asparagine, (2) a precursor of nitric oxide, a diffusible gas regulator of the NMDA receptor, L-arginine, (3) amino acids acting at the glycine site of the NMDA receptor, glycine and D-serine, and a potential precursor for these NMDA co-agonists, L-serine, and (4) other amino acids including a putative inhibitory neurotransmitter, taurine, and neutral amino acids, L-threonine and L-alanine, whose interactions with the NMDA receptor are not unknown. Results represent the mean with SEM of the data obtained from 6-17 aminals. *$p < 0.05$, **$p < 0.01$ as compared to respective saline-treated controls.

Table 2 Effects of acute injection of psychostimulant or antipsychotic on the net concentrations of various amino acids in the rat striatum at 60 min post-injection

	Amino acid concentration (μmol/g of wet weight)				
	NMDA receptor-related amino acids				
	Glutamate site				Nitric oxide
Injection (mg/kg, s.c. or i.p.)	L-Glu	L-Gln	L-Asp	L-Asn	L-Arg
Saline	12.2±0.1	5.86±0.07	2.57±0.05	0.107±0.001	0.141±0.003
MAP (1.6)	12.5±0.1	5.68±0.07	2.26±0.03	0.117±0.001	0.146±0.003
MAP (3.2)	12.7±0.2*	5.52±0.04**	2.25±0.21	0.134±0.009**	0.190±0.014**
MAP (4.0)	13.2±0.1**	5.33±0.08**	2.40±0.05	0.165±0.005**	0.236±0.009**
PCP (7.5)	12.4±0.1	5.66±0.07*	2.26±0.03*	0.109±0.002	0.160±0.005
HAL (1.0)	11.5±0.1**	6.14±0.14*	2.31±0.03	0.109±0.001	0.136±0.004
CLZ (10.0)	11.2±0.1**	6.02±0.09	2.54±0.03	0.105±0.002	0.133±0.005

	Amino acid concentration (μmol/g of wet weight)					
	NMDA receptor-related amino acids					
	Glycine site			Other amino acids		
Injection (mg/kg, s.c. or i.p.)	Gly	D-Ser	L-Ser	Tau	L-Thr	L-Ala
Saline	0.825±0.009	0.236±0.002	0.697±0.007	8.97±0.08	0.620±0.006	0.695±0.013
MAP (1.6)	0.850±0.014	0.244±0.003	0.734±0.008	8.95±0.07	0.661±0.015	0.879±0.020**
MAP (3.2)	0.877±0.025	0.230±0.002	0.754±0.023	8.99±0.08	0.644±0.021	0.943±0.020**
MAP (4.0)	0.964±0.012**	0.237±0.003	0.815±0.019**	8.68±0.06**	0.700±0.020**	0.926±0.016**
PCP (7.5)	0.832±0.007	0.232±0.002	0.692±0.014	9.03±0.07	0.641±0.009	0.769±0.014*
HAL (1.0)	0.828±0.012	0.226±0.003	0.705±0.007	8.74±0.09	0.631±0.017	0.729±0.014
CLZ (10.0)	0.841±0.018	0.221±0.002*	0.690±0.007	8.92±0.06	0.600±0.010	0.653±0.014

Rats were treated with a subcutaneous injection of saline, MAP or PCP, or an intraperitoneal injection of HAL or CLZ acutely, and were killed 60 min thereafter. The amino acids quantified in this study are divided into the following four groups that are defined as indicated in the subheading of Table 1. Results represent the mean with SEM of the data from 6-15 animals.
*$p < 0.05$, **$p < 0.01$ as compared to respective saline-treated controls.

Table 3 Effects of acute injection of psychostimulant or antipsychotic on the ratios of L-Asn/L-Asp and L-Gln/L-Glu in the rat brain at 60 min post-injection

	Neocortex		Striatum	
Injection (mg/kg, s.c. or i.p.)	L-Asn/L-Asp	L-Gln/L-Glu	L-Asn/L-Asp	L-Gln/L-Glu
Saline	0.032±0.001	0.358±0.003	0.041±0.001	0.478±0.007
MAP (1.6)	0.038±0.001	0.321±0.003*	0.051±0.001	0.441±0.006
MAP (3.2)	0.048±0.002**	0.323±0.005*	0.058±0.008**	0.428±0.006**
MAP (4.0)	0.048±0.001**	0.316±0.010**	0.067±0.002**	0.389±0.003**
PCP (7.5)	0.036±0.001	0.352±0.008	0.048±0.001	0.449±0.005
HAL (1.0)	0.030±0.001	0.389±0.014	0.046±0.001	0.534±0.012
CLZ (10.0)	0.028±0.001	0.394±0.012*	0.041±0.001	0.520±0.009

Rats were treated with a subcutaneous injection of saline, MAP or PCP, or an intraperitoneal injection of HAL or CLZ acutely, and were killed 60 min thereafter. Results represent the mean with SEM of the data obtained from 6-17 animals.
*$p < 0.05$, **$p < 0.01$ as compared to respective saline-treated controls.

Table 4 Effects of acute injection of psychostimulant or antipsychotic on the net concentrations of various amino acids in the rat neocortex at 360 min post-injection

	Amino acid concentration (μmol/g of wet weight)				
	NMDA receptor-related amino acids				
	Glutamate site				Nitric oxide
Injection (mg/kg, s.c. or i.p.)	L-Glu	L-Gln	L-Asp	L-Asn	L-Arg
Vehicle	10.5±0.1	5.19±0.07	3.06±0.05	0.106±0.003	0.110±0.003
MAP (4.0)	10.6±0.1	5.33±0.07	3.16±0.09	0.110±0.003	0.101±0.002*
HAL (1.0)	10.2±0.1	5.24±0.18	3.18±0.03	0.109±0.003	0.111±0.003
CLZ (10.0)	10.4±0.1	5.14±0.10	3.24±0.06	0.108±0.002	0.109±0.003

	Amino acid concentration (μmol/g of wet weight)					
	NMDA receptor-related amino acids					
	Glycine site			Other amino acids		
Injection (mg/kg, s.c. or i.p.)	Gly	D-Ser	L-Ser	Tau	L-Thr	L-Ala
Vehicle	0.722±0.020	0.242±0.003	0.740±0.010	5.82±0.07	0.564±0.010	0.628±0.020
MAP (4.0)	0.732±0.038	0.239±0.003	0.794±0.044	5.60±0.08	0.527±0.009*	0.651±0.020
HAL (1.0)	0.740±0.023	0.241±0.004	0.774±0.017	5.66±0.10	0.561±0.013	0.606±0.011
CLZ (10.0)	0.735±0.020	0.237±0.004	0.729±0.017	5.72±0.08	0.531±0.015	0.601±0.016

Rats were treated with a subcutaneous injection of vehicle or MAP, or an intraperitoneal injection of HAL or CLZ acutely, and were killed 360 min thereafter. The amino acids quantified in this study are divided into the following four groups that are defined as indicated in the subheading of Table 1. Results represent the mean with SEM of the data obtained from 6-14 animals. *$p < 0.05$ as compared to respective saline-treated controls.

the content of L-Asn and L-Arg up to 152 and 181% respectively, at 60 min after injection (Table 1). The levels of L-Glu, L-Ser, Gly, L-Ala and L-Thr were also raised, and those of L-Gln were reduced by the MAP treatment, although the magnitude of these changes was small (Table 1). There were no MAP-induced alterations in the concentrations of D-Ser and Tau. An acute subcutaneous injection of PCP induced a significant decrease in L-Asp content without any effects on the other amino acids studied 60 min thereafter (Table 1).

In the striatum (Table 2), the MAP regimen produced a prominent increase in the content of L-Asn, L-Arg and L-Ala by 54, 67 and 33% respectively, and modest changes occurred in the levels of L-Glu (+ 9%), L-Gln (− 9%), L-Ser (+ 17%), L-Thr (+ 13%), Gly (+ 17%) and Tau (− 3%). No significant alterations were observed in L-Asp and D-Ser content following the three doses of MAP (Table 2). PCP at a subcutaneous dose of 7.5 mg/kg diminished L-Asp and L-Gln concentrations, raised L-Ala levels and failed to affect the other amino acid contents examined.

As an index of excitatory amino acid metabolism, we calculated the ratio of L-Asn to L-Asp concentration and of L-Gln to L-Glu concentration. In the neocortex and striatum, acute MAP injection markedly increased the L-Asn/L-Asp ratio and decreased the L-Gln/L-Glu ratio 60 min thereafter, whereas PCP did not have significant effects on these ratios (Table 3).

Neither HAL nor CLZ altered the net neocortical concentrations of the amino acids studied (Table 1). However, these antipsychotics slightly reduced the striatal L-Glu content (Table 2), CLZ produced a very limited modification in the neocortical L-Gln/L-Glu ratio (Table 3) and in the striatal D-Ser content (Table 2), and HAL slightly increased striatal L-Gln levels.

Effects of acute injection of MAP, HAL and CLZ on the net contents of various amino acids in the rat neocortex and striatum at 360 min after injection

As indicated in Tables 4 and 5, 360 min after administration of MAP (4.0 mg/kg, s.c.), HAL (1.0 mg/kg, i.p.) or CLZ (10.0 mg/kg, i.p.) only minimal changes were observed in the net amino acid levels in the neocortex and striatum: (1) MAP decreased neocortical L-Thr (− 7%) and L-Arg (− 8%), and striatal L-Thr (− 7%) content with no significant effects on the other amino acid concentrations in the two brain areas; (2) HAL induced a slight but significant reduction in striatal L-Asp

Table 5 Effects of acute injection of psychostimulant or antipsychotic on the net concentrations of various amino acids in the rat striatum at 360 min post-injection

	Amino acid concentration (μmol/g of wet weight)				
	NMDA receptor-related amino acids				
	Glutamate site				Nitric oxide
Injection (mg/kg, s.c. or i.p.)	L-Glu	L-Gln	L-Asp	L-Asn	L-Arg
Vehicle	9.71±0.15	5.54±0.11	2.06±0.05	0.098±0.003	0.131±0.004
MAP (4.0)	9.68±0.18	5.53±0.17	2.10±0.06	0.095±0.002	0.126±0.003
HAL (1.0)	9.54±0.12	5.95±0.16	1.85±0.05**	0.103±0.001	0.133±0.004
CLZ (10.0)	9.55±0.13	5.39±0.08	2.16±0.03	0.099±0.002	0.135±0.003

	Amino acid concentration (μmol/g of wet weight)					
	NMDA receptor-related amino acids					
	Glycine site			Other amino acids		
Injection (mg/kg, s.c. or i.p.)	Gly	D-Ser	L-Ser	Tau	L-Thr	L-Ala
Vehicle	0.655±0.018	0.210±0.003	0.605±0.010	8.07±0.07	0.566±0.013	0.625±0.010
MAP (4.0)	0.637±0.014	0.209±0.005	0.604±0.012	7.74±0.20	0.526±0.012*	0.656±0.032
HAL (1.0)	0.650±0.015	0.214±0.007	0.618±0.016	8.03±0.19	0.572±0.008	0.676±0.016
CLZ (10.0)	0.658±0.012	0.204±0.005	0.603±0.021	8.04±0.19	0.523±0.010*	0.606±0.012

Rats were treated with a subcutaneous injection of vehicle or MAP, or an intraperitoneal injection of HAL or CLZ acutely, and were killed 360 min thereafter. The amino acids quantified in this study are divided into the following four groups that are defined as indicated in the subheading of Table 1. Results represent the mean with SEM of the data obtained from 6-14 animals. *$p < 0.05$, **$p < 0.01$ as compared to respective saline-treated controls.

Table 6 Effects of acute injection of psychostimulant or antipsychotic on the ratios of L-Asn/L-Asp and L-Gln/L-Glu in the rat brain at 360 min post-injection

	Neocortex		Striatum	
Injection (mg/kg, s.c. or i.p.)	L-Asn/L-Asp	L-Gln/L-Glu	L-Asn/L-Asp	L-Gln/L-Glu
Vehicle	0.030±0.001	0.545±0.006	0.050±0.001	0.623±0.009
MAP (4.0)	0.031±0.001	0.559±0.009	0.049±0.002	0.614±0.016
HAL (1.0)	0.029±0.001	0.584±0.024	0.059±0.002**	0.686±0.030
CLZ (10.0)	0.028±0.001	0.545±0.008	0.048±0.001	0.620±0.017

Rats were treated with a subcutaneous injection of vehicle, MAP or PCP, or an intraperitoneal injection of HAL or CLZ acutely, and were killed 360 min thereafter. Results represent the mean with SEM of the data obtained from 6-14 animals.
**$p < 0.01$ as compared to respective saline-treated controls.

levels without affecting the levels of other amino acids in the neocortex and striatum; and (3) CLZ produced no changes except for a reduction in striatal L-Thr levels.

There were no significant changes in the L-Asn/L-Asp and L-Gln/L-Glu ratios in the neocortex and striatum 360 min after systemic MAP, HAL or CLZ application, except HAL-induced augmentation in striatal L-Asn/L-Asp ratios (Table 6).

Effects of pretreatment with HAL or CLZ on the net content of various amino acids in the rat neocortex and striatum 60 min after acute injection of MAP

In the neocortex and the striatum, pretreatment with HAL (1.0 mg/kg, i.p.) and CLZ (10.0 mg/kg, i.p.) attenuated the ability of MAP (4.8 mg/kg, s.c.) to augment L-Arg (Fig. 1) and L-Asn (Fig. 2) levels (Table 7 and 8). The MAP-induced increase in the neocortical, but not striatal, L-Asn/

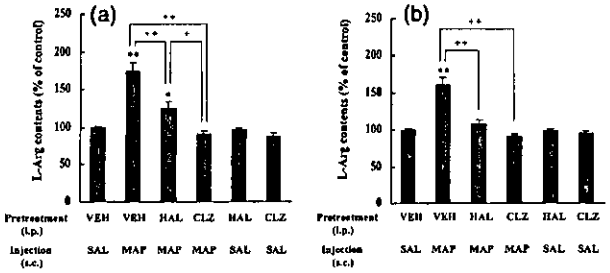

Fig. 1 Effects of intraperitoneal injection of HAL or CLZ on the ability of MAP to increase levels of L-Arg in the (a) neocortex and (b) striatum of the rat. MAP (4.8 mg/kg, s.c.) or saline (SAL) was administered 60 min, and HAL (1 mg/kg, i.p.), CLZ (10 mg/kg, i.p.) or vehicle (VEH) was injected 90 min, before the animal was killed. Results are mean ± SEM values from 6–16 animals and are expressed as a percentage of control values, which were: neocortex, 0.107 ± 0.002 μmol per g tissue; striatum, 0.136 ± 0.003 μmol per g. $^{*}p < 0.05$, $^{**}p < 0.01$ versus vehicle-treated saline-injected controls. $+p < 0.05$, $++p < 0.01$ (ANOVA followed by Scheffé post-hoc test).

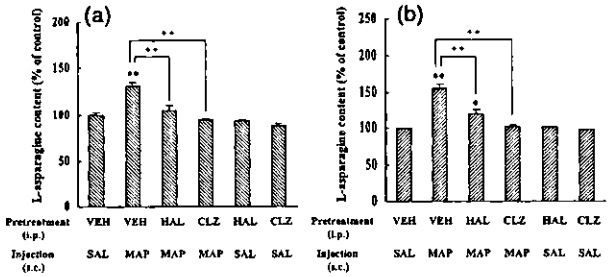

Fig. 2 Effects of intraperitoneal injection of HAL or CLZ on the ability of MAP to increase levels of L-Asn in (a) neocortex and (b) striatum of the rat. MAP (4.8 mg/kg, s.c.) or saline (SAL) was administered 60 min, and HAL (1 mg/kg, i.p.), CLZ (10 mg/kg, i.p) or vehicle (VEH) was injected 90 min, before the animal was killed. Results are the mean ± SEM of values obtained from 6–16 animals and are expressed as a percentage of control values, which were: neocortex, 0.128 ± 0.003 μmol per g tissue; striatum, 0.107 ± 0.001 μmol per g. $^{*}p < 0.05$, $^{**}p < 0.01$ versus vehicle-treated saline-injected controls. $++p < 0.01$ (ANOVA followed by Scheffé post-hoc test).

L-Asp ratio was inhibited by HAL and CLZ (Table 9). CLZ tended to produce a greater antagonism of the effects of MAP than HAL (Figs 1 and 2; Tables 7 and 8). Indeed, the levels of neocortical L-Arg after MAP in combination with CLZ were significantly lower than those after MAP with HAL (Fig. 1a).

The MAP-induced increase in neocortical L-Thr content was also reversed by CLZ pretreatment, whereas neither HAL nor CLZ significantly inhibited the reduction in L-Asp content (Table 7) and in the L-Gln/L-Glu ratios (Table 9), or the increase in L-Glu levels (Table 7). In the striatum, HAL or CLZ given systemically 30 min before MAP injection blocked the up-regulation by MAP of the concentrations of L-Glu, L-Ser, L-Thr, Gly and L-Ala (Table 8). CLZ, but not HAL, attenuated the MAP-induced decrease in the L-Gln/L-Glu ratio (Table 9).

Discussion

The basal values obtained here for tissue concentrations of neocortical and striatal amino acids are compatible with those in our previous studies (Hashimoto *et al.* 1992b; Takahashi *et al.* 1997) and other reports (Ramirez de Guglielmone and Gomez 1966; Tossman *et al.* 1986). These results support the reliability of our assay method for amino acids.

The present study is the first to demonstrate that acute systemic administration of MAP, a schizophrenomimetic, markedly augments the net concentrations of L-Arg and L-Asn in the neocortex and striatum in a antipsychotic-reversible fashion. Moreover, MAP induction of the striking increase in neocortical, but not striatal, L-Asn/L-Asp ratios is attenuated by HAL and CLZ treatment. MAP also produces a slight-to-moderate and HAL- and/or CLZ-sensitive increase in levels of neocortical L-Thr and of striatal L-Glu, L-Ser, L-Thr, Gly and L-Ala. A MAP-induced small reduction in L-Gln/L-Glu ratio in the neocortex is insensitive to the two antipsychotics, whereas that in the striatum is sensitive to CLZ, but not HAL.

These phenomena do not seem to be due to an artifact because PCP, another schizophrenomimetic with a pharmacological profile distinct from that of MAP, did not alter the net content of the amino acids quantified, apart from a decrease in L-Asp levels in the neocortex and striatum. Reduced L-Asp levels in the striatum were also noted by Yonezawa *et al.* (1992). These differences could, at least in part, underlie differences in behavioral or psychotomimetic effects between MAP and PCP.

Only slight alterations in the concentrations of a few amino acids in the neocortex and striatum of MAP-treated rats were observed 360 min after injection, suggesting that the effects of MAP on cerebral amino acids are relatively short lasting. Because HAL is a D2-preferring dopamine receptor antagonist (Miyamoto *et al.* 2002), the HAL-sensitive nature of MAP-induced changes in cortical L-Arg and L-Asn and in striatal L-Arg, L-Asn, L-Glu, Gly, L-Ser, L-Thr and L-Ala supports the idea that these changes are likely to be associated with increased dopaminergic neurotransmission owing to the facilitation of release and inhibition of reuptake of dopamine by MAP (Seiden *et al.* 1993).

This theory seems to be consistent with the observation using an *in vivo* dialysis technique that application of exogenous L-Arg via the dialysis tubing augments extracellular dopamine concentrations in the striatum (Strasser *et al.* 1994), indicating an interaction between L-Arg and the dopaminergic system. The fact that MAP- and L-Arg-induced striatal dopamine release is eliminated by a NO synthase inhibitor N^{G}-nitro-L-arginine methyl ester (L-NAME) and that some behavioral effects of MAP are blocked by L-NAME (Ohno and

Table 7 Effects of acute MAP injection on the net concentrations of neocortical various amino acids in the rats pretreated with HAL or CLZ

		Amino acid concentration (μmol/g of wet weight)				
		NMDA receptor-related amino acids				
		Glutamate site				Nitric oxide
Pretreatment (mg/kg i.p.)	Injection (mg/kg, s.c.)	L-Glu	L-Gln	L-Asp	L-Asn	L-Arg
Vehicle	Saline	15.5±0.2	5.48±0.06	3.80±0.05	0.138±0.003	0.107±0.002
Vehicle	MAP (4.8)	17.7±0.2**	5.41±0.06	3.49±0.06*	0.180±0.007**	0.186±0.014**
HAL (1.0)	MAP (4.8)	17.2±0.2**	5.32±0.07	3.51±0.04*	0.145±0.006++	0.134±0.011*,++
CLZ (10.0)	MAP (4.8)	16.6±0.1**	5.51±0.11	3.31±0.03**	0.130±0.002++	0.097±0.006**,#
HAL (1.0)	Saline	15.0±0.1	5.58±0.06	3.88±0.07	0.136±0.002	0.113±0.003
CLZ (10.0)	Saline	14.9±0.2	5.79±0.13	3.84±0.13	0.130±0.002	0.096±0.002

		Amino acid concentration (μmol/g of wet weight)					
		NMDA receptor-related amino acids					
		Glycine site			Other amino acids		
Pretreatment (mg/kg i.p.)	Injection (mg/kg, s.c.)	Gly	D-Ser	L-Ser	Tau	L-Thr	L-Ala
Vehicle	Saline	1.05±0.02	0.266±0.003	1.09±0.02	6.15±0.06	0.666±0.009	0.748±0.011
Vehicle	MAP (4.8)	1.11±0.03	0.275±0.006	1.16±0.03	6.17±0.12	0.770±0.018**	0.816±0.011**
HAL (1.0)	MAP (4.8)	1.06±0.02	0.276±0.003	1.09±0.02	6.15±0.07	0.705±0.012	0.789±0.010
CLZ (10.0)	MAP (4.8)	1.00±0.03	0.272±0.004	1.03±0.03++	6.13±0.10	0.683±0.018++	0.766±0.011
HAL (1.0)	Saline	1.02±0.01	0.268±0.003	1.09±0.01	6.21±0.10	0.661±0.012	0.726±0.013
CLZ (10.0)	Saline	1.05±0.01	0.264±0.003	1.08±0.02	6.14±0.04	0.651±0.014	0.755±0.010

MAP or saline was administered 60min, and HAL, CLZ or vehicle was injected 90 min before sacrifice. The amino acids quantified in this study are divided into the following four groups that are defined as indicated in the subheading of Table I. Results represent the mean with SEM of the data obtained from 7-16 animals. $^{*}p < 0.05$, $^{**}p < 0.01$ compared to vehicle-pretreated saline-injected controls. $^{++}p < 0.01$ compared to vehicle-pretreated MAP-injected animals. $^{\#}p < 0.05$, compared to haloperidol-pretreated MAP-injected animals.

Watanabe 1995; Inoue *et al.* 1996) raises the possibility that the stimulatory effect of MAP on striatal L-Arg levels may lead to augmented dopamine release owing to overproduction of NO from the increased L-Arg by neural NO synthase. Moreover, previous observations of an MAP-induced increase in extracellular L-Glu levels in the frontal cortex (Shoblock *et al.* 2003) and striatum (Zhang *et al.* 2001) and of NMDA receptor-mediated activation of the NO-generating system (Southam *et al.* 1991) allow us to postulate that the increased levels of neocortical and striatal L-Glu after MAP administration in this study might stimulate NO synthesis through an increased extracellular release of L-Glu and NMDA receptor stimulation. The plausible metabolic links among L-Arg, NO, L-Glu NMDA receptor and dopamine might represent an additional mechanism underlying MAP-induced hyperdopaminergic activity. These data suggest that an increase in neocortical and striatal L-Glu as well L-Arg following acute MAP administration would also be connected to the interaction between dopamine and the NO system.

Our results concerning L-Asn levels and L-Asn/L-Asp ratios indicate that L-Asn metabolism might be under dopaminergic regulation in the neocortex and striatum. This regulation appears to be related to the cerebral dopamine–excitatory amino acid interaction, because (i) an excitatory amino acid L-Asp is shown to be formed by deamination of L-Asn which is catalysed by the enzyme asparaginase in rat brain (Dieterich *et al.* 2003), (ii) [^{14}C]Asn has been reported to be converted to a great extent to [^{14}C]Asp which is decreased by lesioning of cortico-striatal pathways (Reubi *et al.* 1980), and (iii) evidence has accumulated indicating that the excitatory amino acid system including L-Asp, L-Glu and NMDA co-agonists Gly and D-Ser have mutual interactions with dopaminergic systems in the cortical and subcortical brain areas through the NMDA or non-NMDA ionotropic or metabotropic Glu receptors (Nishijima *et al.* 1994; 1996; Umino *et al.* 1998; Sesack *et al.* 2003). Interruption of excitatory amino acid transmission via the NMDA receptor has been observed to inhibit the development of behavioral sensitization induced by amphetamines